

UC Davis

UC Davis Previously Published Works

Title

A conceptual geochemical model of the geothermal system at Surprise Valley, CA

Permalink

<https://escholarship.org/uc/item/3f31s797>

Journal

Journal of Volcanology and Geothermal Research, 353

ISSN

0377-0273

Authors

Fowler, APG
Ferguson, C
Cantwell, CA
[et al.](#)

Publication Date

2018-03-15

DOI

10.1016/j.jvolgeores.2018.01.019

Peer reviewed

A conceptual geochemical model of the geothermal system at Surprise Valley, CA

Author links open overlay panel [Andrew P.G.Fowler^a](#) [Colin Ferguson^a](#) [Carolyn A.Cantwell^a](#) [Robert A.Zierenberg^a](#) [James McClain^a](#) [Nicolas Spycher^a](#) [Patrick Dobson^b](#)

Show more

<https://doi.org/10.1016/j.jvolgeores.2018.01.019> Get rights and content

Highlights

-

A conceptual geochemical model of the Surprise Valley geothermal system is presented

-

Optimized multicomponent geothermometry suggests thermal springs equilibrated at progressively lower temperatures

-

Thermal springs have D/H values lower than any modern cold recharge source

Abstract

Characterizing the [geothermal system](#) at Surprise Valley (SV), northeastern California, is important for determining the sustainability of the [energy resource](#), and mitigating hazards associated with hydrothermal eruptions that last occurred in 1951. Previous geochemical studies of the area attempted to reconcile different hot spring compositions on the western and eastern sides of the valley using scenarios of dilution, equilibration at low [temperatures, surface](#) evaporation, and differences in rock type along flow paths. These models were primarily supported using classical [geothermometry](#) methods, and generally assumed that fluids in the Lake City [mud volcano](#) area on the western side of the valley best reflect the composition of a deep geothermal fluid. In this contribution, we address controls on hot spring compositions using a different suite of geochemical tools, including optimized multicomponent [geochemistry](#) (GeoT) models, hot spring fluid major and [trace element](#) measurements, mineralogical observations, and [stable isotope](#) measurements of hot spring fluids and precipitated carbonates. We synthesize the results into a conceptual geochemical model of the Surprise Valley geothermal system, and show that high-temperature (quartz, Na/K, Na/K/Ca) classical geothermometers fail to predict maximum subsurface temperatures because fluids re-

equilibrated at progressively lower temperatures during outflow, including in the Lake City area. We propose a model where hot spring fluids originate as a mixture between a deep thermal brine and modern meteoric fluids, with a seasonally variable [mixing ratio](#). The deep brine has [deuterium](#) values at least 3 to 4‰ lighter than any known groundwater or high-elevation snow previously measured in and adjacent to SV, suggesting it was recharged during the Pleistocene when meteoric fluids had lower deuterium values. The deuterium values and compositional characteristics of the deep brine have only been identified in thermal springs and groundwater samples collected in proximity to structures that transmit thermal fluids, suggesting the brine may be thermal in nature. On the western side of the valley at the Lake City mud volcano, the deep brine-meteoric water mixture subsequently boils in the shallow subsurface, precipitates [calcite](#), and re-equilibrates at about 130 °C. On the eastern side of the valley, meteoric fluid mixes to a greater extent with the deep brine, cools conductively without boiling, and the composition is modified as dissolved elements are sequestered by [secondary minerals](#) that form along the cooling and outflow path at temperatures <130 °C. Re-equilibration of geothermal fluids at lower temperatures during outflow explains why subsurface temperature estimates based on classical geothermometry methods are highly variable, and fail to agree with temperature estimates based on dissolved sulfate-oxygen isotopes and results of classical and multicomponent geothermometry applied to reconstructed deep well fluids. The proposed model is compatible with the idea suggested by others that thermal fluids on the western and eastern side of the valley have a common source, and supports the hypothesis that low temperature re-equilibration during west to east flow is the major control on hot spring [fluid compositions](#), rather than dilution, evaporation, or differences in rock type.

Keywords

Surprise Valley

Geothermal

Geochemical modeling

Optimized multicomponent geothermometry

Rare earth elements

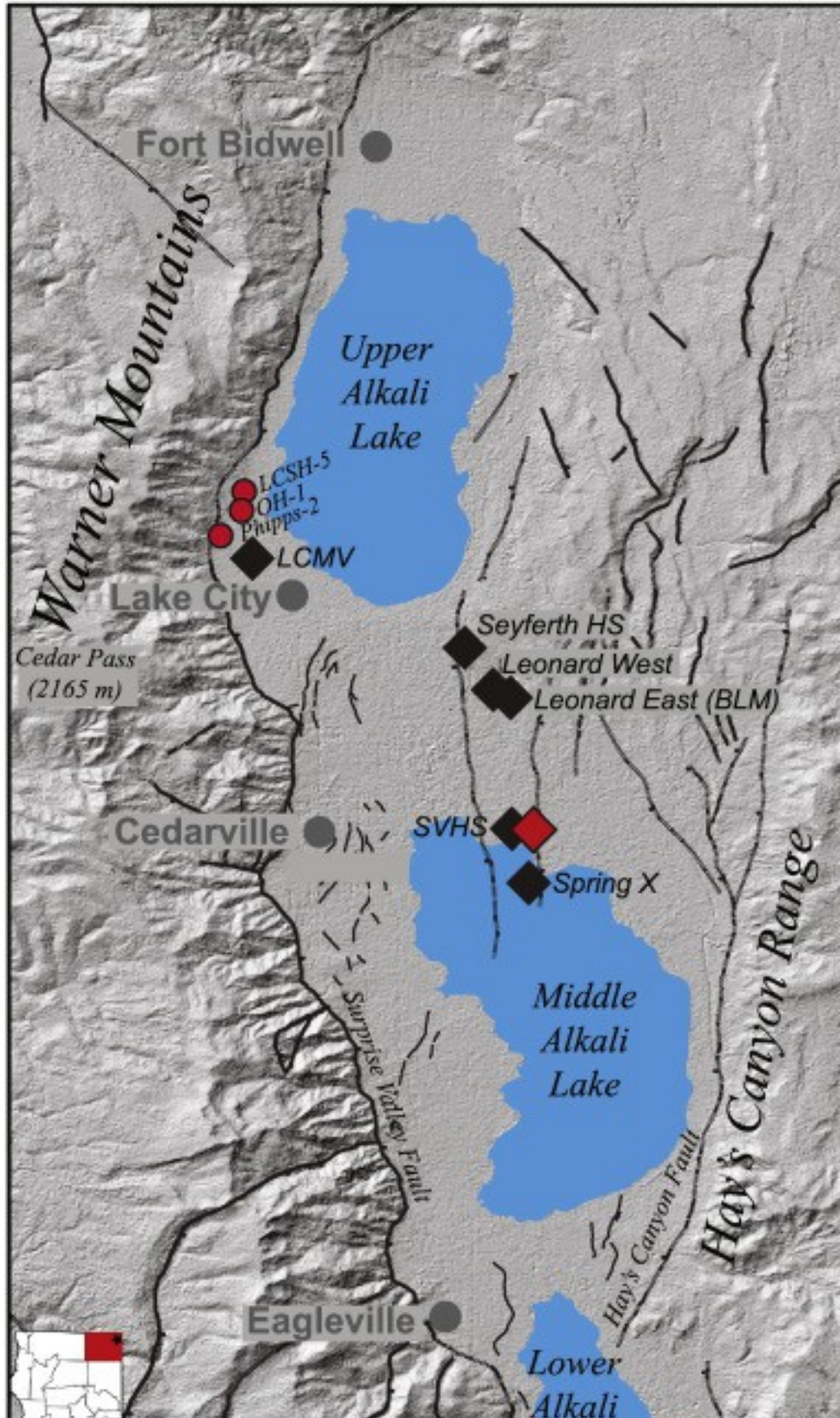
Trace elements

1. Introduction

Surprise Valley, northeastern California, is an active geothermal area located on the western edge of the Basin and Range extensional province and at the northern terminus

of the Walker Lane dextral-slip belt ([Egger et al., 2010](#)). Hot and warm springs occur throughout the valley; the main locations are near Eagleville, Lake City, and Fort Bidwell on the western side; and at the Surprise Valley Hot Springs Resort (SVHS), Leonards hot spring, and Seyferth hot spring on the eastern side of the valley ([Fig. 1](#)).

Geochemical studies related to energy exploration of the geothermal areas in Surprise Valley have been conducted periodically since the 1950s. The purpose of this study is to revisit the conceptual geochemical model of the Surprise Valley [geothermal system](#), taking advantage of the large body of historical data, advances in geochemical modeling software, and accessibility to high-resolution [trace element](#) analytical data.



1. [Download high-res image \(2MB\)](#)
2. [Download full-size image](#)

Fig. 1. Surprise Valley showing sampling locations. Spring E of SVHS (northern and southern) and Spring SW of SVHS (see [Table 1](#)) are located adjacent to SVHS.

1.1. Background

Direct use of the Surprise Valley [geothermal resource](#) began in the 1950s with construction of the SVHS, where boiling water from a 27 m deep well is still used to heat spas. Interest in the [geothermal energy](#) potential of Surprise Valley followed eruption of the Lake City [mud volcano](#) (LCMV) in March 1951 on the western side of the valley ([White, 1955](#)). [Magma](#) Energy, Inc. subsequently drilled three exploratory wells in the LCMV area between 1959 and 1962. Parman-1 reached 140 °C at 655 m, Parman-2 reached 125 °C at 600 m depth, and Parman-3 reached 92 m when a blowout destroyed the rig and expelled boiling water ([Woods, 1974](#); [Reed, 1975](#)). Following designation of Lake City as a known geothermal resource area (KGRA) under the Geothermal Steam Act of 1970 ([Godwin et al., 1971](#)), six more deep [test wells](#) were drilled by Magma Energy, Inc., Gulf Oil Corporation, and American Thermal Resources between 1970 and 1974. This included the 1508 m deep Phipps-2 exploration well just to the northwest of LCMV, which achieved the maximum measured subsurface temperature in the valley of between 160 °C and 170 °C ([Duffield and Fournier, 1974](#); [Rigby and Zebal, 1981](#)).

A lack of local demand for hot water and electricity led to a hiatus in Surprise Valley geothermal exploration ([Rigby and Zebal, 1981](#)) until the 2000s, when interest in the Surprise Valley geothermal resource renewed. A series of temperature gradient and core holes were drilled in the LCMV ([Benoit et al., 2004](#); [Benoit et al., 2005a](#); [Benoit et al., 2005b](#)) and Fort Bidwell ([Barker et al., 2005](#); [LaFleur et al., 2010](#)) areas. During these efforts, holes OH-1 and LCSH-5 were drilled to the north of Phipps-2 and near the Surprise Valley Fault (SVF). OH-1 and LCSH-5 were drilled to 1047 m and 1441 m, respectively, and the wells both achieved maximum temperatures of approximately 160 °C during testing, comparable to the bottom hole temperature measured in Phipps-2 ([Benoit et al., 2005b](#)). In 2016, the California Energy Commission (CEC) funded drilling of three closely spaced temperature gradient holes on the eastern side of the valley near SVHS, including one for which water samples were collected. The results of [water sampling](#) from the [CEC](#) project are discussed herein.

In addition to exploration drilling, several geophysical and geologic studies have been conducted to evaluate geologic and [structural controls](#) on subsurface geothermal [fluid flow](#) in Surprise Valley using high-quality gravity, magnetic, and audio magnetotelluric

measurements ([Glen et al., 2008](#); [Kell-Hills et al., 2009](#); [Lerch et al., 2010](#); [Glen et al., 2013](#); [Hawkes et al., 2013](#); [Egger et al., 2014](#); [Athens et al., 2016](#); [Tanner et al., 2016](#)). These studies show a close association of hot springs with faults in Surprise Valley, and support the contention of [Duffield and Fournier \(1974\)](#) that thermal fluid flow is structurally controlled ([Egger et al., 2014](#)). A dominant structural control on thermal fluid flow appears to be the SVF, a major offset [normal fault](#) located along the eastern front of the Warner Mountains ([Duffield and McKee, 1986](#); [Egger et al., 2010](#)). A number of authors (e.g. [Glen et al., 2013](#)) argued for the existence of a northwest striking “Lake City Fault” connecting the Lake City [hydrothermal system](#) with the system on the east side of the valley. [Hawkes et al. \(2013\)](#) argue against a major fault in this location based on audiomagnetic studies. [Egger et al. \(2014\)](#) also found little evidence for a distinct ‘Lake City Fault’, and instead proposed a model where small offset N-S trending and westward dipping normal faults intersect the SVF at depth and facilitate flow of [thermal waters](#) to the eastern side of the valley. Magnetotelluric surveys conducted by [Tanner et al. \(2016\)](#) recognized that hot spring locations fall off-axis of the westward dipping faults identified by [Egger et al. \(2014\)](#), and proposed that porous [basalts](#) within fault-tilted blocks provide a fluid pathway. [Fowler et al. \(2017\)](#) identified two distinct groundwater trends with a thermal signature using a statistical analysis of historical groundwater geochemical data. One subsurface trend is coincident with the SVF on the western side of the valley between Lake City and Fort Bidwell, and the other trend is located on the eastern side of the valley and is coincident with the trend of the small N-S trending westward dipping faults and porous basalts.

Renewed interest in the Surprise Valley geothermal resource provides a need to revisit geochemical models of the geothermal system. Conceptual geochemical models of the Surprise Valley geothermal system have been based on classical [geothermometry](#) calculations, which rely upon variations of dissolved concentrations as a function of temperature. We refer to classical geothermometers as the empirical and [thermodynamic](#) temperature-solubility relations for [silica](#), [feldspar](#) and micas, termed the [quartz](#), [chalcedony](#), Na/K, and Na/K/Ca geothermometers (e.g. [Fournier, 1977](#); [Giggenbach, 1988](#)). All geothermometer relations are dependent on the assumptions that: 1) dissolved concentrations reflect fluid-mineral equilibrium at the maximum subsurface temperature, 2) fluids did not re-equilibrate at lower temperatures along the outflow path, and 3) there was no mixing with fluids of a different composition ([Fournier, 1977](#)). Additional caveats apply to specific geothermometers; however, it is beyond the scope of this study to review and reiterate these details. Temperature agreement between several different geothermometer formulations is

generally thought to indicate that these assumptions are robust. When these geothermometers disagree, the primary assumptions must be revisited. Previous studies of the Surprise Valley geothermal system have utilized discrepancies between results for various classical geothermometers to propose conceptual geochemical models of dilution or low temperature re-equilibration.

[Duffield and Fournier \(1974\)](#) proposed that conservative element concentrations indicate LCMV fluids are undiluted outflow of deep geothermal fluids that equilibrated between 153 °C to 174 °C based on quartz and Na-K-Ca geothermometer temperature estimates, while fluids on the eastern side of the valley are diluted by low-concentration [meteoric water](#). When corrected for dilution, the calculations suggested that the SVHS fluids equilibrated between 135 °C and 145 °C, and Leonard's hot spring fluids equilibrated between 170 °C and 185 °C.

[Reed \(1975\)](#) reported a range of inferred subsurface temperatures for hot springs throughout Surprise Valley using several classical geothermometry formulations without making any corrections for dilution, and estimated a maximum resource temperature of 200 °C to 205 °C based on dissolved sulfate [oxygen isotope](#) measurements of SVHS and Seyferth hot spring fluids. [Mariner et al. \(1993\)](#) showed that the dissolved sulfate oxygen isotope geothermometer indicates higher temperatures than [cation](#) geothermometers in a study of geothermal waters from the broader Modoc Plateau region, and included the [Reed \(1975\)](#) samples from SVHS and Seyferth hot spring in their study. [Mariner et al. \(1993\)](#) suggested that many dissolved constituents, particularly K, Mg, Li, SiO₂, and HCO₃, may have re-equilibrated at intermediate temperatures along the fluid outflow path, and suggested that cation geothermometers may not preserve evidence of maximum subsurface temperatures in many Modoc Plateau waters, including Surprise Valley.

[Sladek et al. \(2004\)](#) presented concentration and [stable isotope](#) data for hot spring fluids from several locations throughout Surprise Valley. They pointed out that conservative element variations in hot spring fluids are actually quite small, and suggested that differences in rock type along flow paths are responsible, rather than effects of dilution. [Sladek et al. \(2004\)](#) also suggested that springs on the eastern side of the valley had partially re-equilibrated at lower temperatures during outflow, and supported this hypothesis by calculating equilibration temperatures using an average of results for the quartz, chalcedony and Na-K-Ca geothermometers. They also argued that δD and $\delta^{18}O$ values of hot spring fluids lie on a line that reflects surface evaporation of springs, and speculated that δD and $\delta^{18}O$ values of [spring waters](#) are influenced by recharge from snow at high elevations, recharge from isotopically light Pleistocene

groundwater, interaction with different rock types along different flow paths, or dilution by groundwater.

[Cantwell and Fowler \(2014\)](#) and [Fowler et al. \(2015\)](#) used published major element data in combination with multicomponent geothermometry modeling techniques to evaluate various dilution and boiling scenarios proposed for Surprise Valley thermal waters. Their models of deep fluids sampled from the Phipps-2 well indicated equilibration temperatures of up to 228 °C, when steam loss and pH changes owing to boiling-induced CO₂ loss were accounted for. The models suggested that thermal springs on the eastern side of the valley could simply have re-equilibrated with a lower temperature mineral assemblage than fluids in the LCMV area, and were not necessarily diluted as suggested by [Duffield and Fournier \(1974\)](#). The models also indicated that only thermal waters from Fort Bidwell could be explained by dilution with low total dissolved solids meteoric water. Their work was unable to address the influence of rock type and evaporation on hot spring [fluid compositions](#), owing to a lack of published fluid trace element and stable isotope data for springs on the eastern side of the valley.

In this contribution, we examine the relationship between thermal springs on the eastern and western side of Surprise Valley using a new and comprehensive geochemical dataset coupled with multicomponent geochemical modeling. We provide analytical and stable isotope data for fluids from the LCMV, Seyferth, Leonards, SVHS, and several small hot springs in the SVHS area. We also present fluid analytical results from a recent California Energy Commission (CEC) funded temperature gradient hole drilled on the eastern side of the valley (hereafter referred to as the CEC borehole). We utilize optimized multicomponent geothermometry (e.g. [Peiffer et al., 2014](#); [Spycher et al., 2014](#)) and corrections for CO₂ loss to model fluid equilibration temperatures, and assess the feasibility of previously proposed models of dilution and low-temperature re-equilibration. We synthesize our results into a conceptual geochemical model of the Surprise Valley geothermal system. We show that dilution is unlikely because unrealistic concentration factors are required to reconstruct deep fluids to reflect equilibrium with a reasonable reservoir mineral assemblage. We suggest that hot spring fluids throughout the valley have re-equilibrated at lower temperatures after undergoing boiling on the west side of the valley at LCMV, and conductive cooling on the east side of the valley in SVHS area springs, Seyferth, and Leonards hot springs. We also identify the geothermal source fluid as a mixture between modern meteoric fluids and a brine with [deuterium](#) values lower than any known modern meteoric waters in the valley and bounding ranges. An important implication of this work is that classical geothermometers (i.e. quartz, chalcedony, Na/K, and Na/K/Ca) applied to surface hot

spring fluid samples do not reflect the maximum geothermal reservoir temperatures in Surprise Valley. Our results show how Surprise Valley thermal fluids can originate from a single source. While distinct compartmentalized geothermal fluid reservoirs cannot be ruled out, they are not required to describe observed compositional variability. Our revised conceptual model provides context to discuss potential triggering mechanisms of the LCMV mud volcano eruption, which presents an unquantifiable hazard without a better understanding of the Surprise Valley geothermal system plumbing.

2. Methods

2.1. Sampling and analysis

Hot spring samples were collected using all-plastic HDPE syringes (NormJect®), dedicated Tygon® tubing, HDPE luer stop-cock valves, and were stored in acid-cleaned HDPE bottles. Samples from the California Energy Commission (CEC) temperature gradient well (TG-2) were sampled from at a depth of 274 m in the auger barrel using the airlift method. Separate sample aliquots were used for field pH and conductivity measurements. Samples for [cation](#) and [trace element](#) analysis were filtered (0.45 µm) and acidified in the field using 1 mL HNO₃ (67–69% Optima™ grade, Fisher Scientific) per 120 mL. Samples for [stable isotope](#), [anion](#), pH and conductivity measurements were filtered in the field, but not acidified. Samples were stored on ice for transport and refrigerated pending analysis. Sampling locations and field measurements are provided on [Table 1](#).

Table 1. Fluid sample locations and field parameters (see [Fig. 1](#) for locations).

Sample ID	Sampling date	Site name	UTM grid	Easting	Northing	Elevation (m)	Temp. (°C)	Field pH	Field conductivity (mS/cm)	Notes
20150824-1	8/24/2015	SVHS Hot Well	10T	743766	4602055	1373	97	8.46	1.372	Boiling
20150824-2	8/24/2015	Spring E of SVHS (northern)	10T	744167	4602264	1377	91	8.29	1.432	
20150824-3	8/24/2015	Spring E of SVHS (southern)	10T	744200	4602174	1371	89	8.20	1.390	
20150824-4	8/24/2015	Spring SW of SVHS	10T	743386	4601797	1368	97	8.17	1.404	Boiling
20150824-5	8/24/2015	Cold water well at Desert Rose	10T	744634	4603365	1369	14	8.47	0.293	
20150824-	8/24/2015	Spring X	10T	744332	4599812	1354	55	9.33	1.520	57 °C in

Sample ID	Sampling date	Site name	UTM grid	Easting	Northing	Elevation (m)	Temp. (°C)	Field pH	Field conductivity (mS/cm)	Notes
6										mud
20150825-1	8/25/2015	Seyferth (chicken) Hot Spring	10T	741317	4611137	1395	83	7.81	1.690	
20150825-2	8/25/2015	Leonard's Hot Spring East	10T	742898	4609625	1381	62	7.85	1.647	
20150825-3	8/25/2015	Leonard's Hot Spring West (BLM)	10T	743354	4609507	1400	69	8.29	1.320	72 °C in mud
20150825-4	8/25/2015	LCMV	10T	732275	4616634	1362	99	7.47	1.721	Boiling
20160321-1	3/21/2016	SVHS Hot Well	10T	743765	4602052	1380	79	8.51	1.505	Could not reach direct discharge
20160321-2	3/21/2016	SVHS Reed Spring	10T	743896	4601867	1372	40	7.95	1.321	
20160321-3	3/21/2016	Spring SW of SVHS	10T	743381	4601796	1375	90	8.12	1.720	Cinnabar Present
20160321-4	3/21/2016	SVHS Flat Shack Spring	10T	742965	4601684	1372	83	8.17	1.573	
20160321-5	3/21/2016	Spring E of SVHS (small)	10T	744193	4602244	1374	76	8.15	1.637	Cinnabar Present
20160321-6	3/21/2016	Spring E of SVHS (northern)	10T	744168	4602263	1374	77	8.06	1.553	
20160321-7	3/21/2016	Spring E of SVHS (tiny)	10T	744170	4602199	1376	68	8.16	1.779	
20160321-8	3/21/2016	Spring E of SVHS (southern)	10T	744194	4602181	1377	82	8.03	1.751	Cinnabar Present
20160321-9	3/21/2016	SVHS Cold Well	10T	743765	4602052	1380	13	8.81	0.367	Sampled at Resort, not wellhead.
20160321-10	3/21/2016	SVHS Hot Wellhead Near Ponds	10T	743602	4602110	1383	81	8.05	1.714	
20161101-1	11/2016	CEC Exploratory Borehole	10T	744164	4602191	1372	~50	–	–	Airlift sample from

Sample ID	Sampling date	Site name	UTM grid	Easting	Northing	Elevation (m)	Temp. (°C)	Field pH	Field conductivity (mS/cm)	Notes
-----------	---------------	-----------	----------	---------	----------	---------------	------------	----------	----------------------------	-------

274 m

SVHS = Surprise Valley Hot Springs.

BLM = Bureau of Land Management.

LCMV = Lake City [Mud Volcano](#).

[CEC](#) Exploratory [Borehole](#) – Recent temperature gradient hole drilled adjacent to SVHS in October 2016. Coordinates and elevations were recorded by [GPS](#) (NAD83), and vary within the limitations of the device used.

Cation and trace element analyses were completed at the University of California (UC Davis) Interdisciplinary Center for Plasma Mass Spectrometry using inductively coupled plasma mass [spectrometry](#) (ICP-MS; Agilent 4500 quadrupole). [Boron](#) and anion (Cl, SO₄, NO₃, HCO₃, and CO₃) measurements; along with sodium, calcium, and magnesium for select samples; were completed by the UC Davis Analytical Laboratory (AnLab) using ICP atomic emission spectrometry (ICP-AES). Laboratory measurements of [electrical conductivity](#) and pH were also completed at AnLab. Fluid stable isotope (oxygen and hydrogen) analyses were completed at the UC Davis Stable Isotope Facility using laser spectroscopy (Los Gatos Instruments) (e.g. [Kerstel et al., 1999](#)). Fluid samples for [rare earth element](#) (REE) analysis were prepared using a modified (offline) version of the [Zhu et al. \(2010\)](#) pre-concentration method, which is described by [Fowler and Zierenberg \(2015\)](#). Analytical accuracy and detection limits for [REE](#) analyses were quantified through repeated analyses of the NASS-6 seawater standard. The detection limit is defined as 3 times the standard deviation of 6 replicate analysis of REE in the NASS-6 seawater standard.

Carbonate blocks ejected from the 1951 LCMV eruption were sampled for stable [carbon isotope](#) ($\delta^{13}\text{C}$ PDB) and [oxygen isotope](#) ($\delta^{18}\text{O}$ SMOW) analysis. [Calcite](#) samples were also collected from a fossil hot spring (FHS) [travertine](#) deposit exposed in a nearby road cut. Calcite samples were observed to have different [crystal](#) habits or distinct generations of growth, as observed in hand sample, in thin section, and using [cathodoluminescence](#) (CL). Different calcite generations and morphologies were sampled using a microdrill. Powdered Carrera Marble standard, and powdered calcite samples were placed under vacuum and roasted at 375 °C to drive off atmospheric or organic material contamination, and a [liquid nitrogen](#) trap was used to capture and remove these contaminants. The powdered, roasted samples were then dissolved in

anhydrous [phosphoric acid](#) at 90 °C under vacuum. Non-condensable gasses and [sulfur](#) were removed by [cryogenic](#) vacuum [distillation](#) using liquid nitrogen and a [pentane slurry](#) at its freezing point in a two-step process. Sealed vacuum tube samples of purified CO₂ gas were then analyzed by [mass spectrometer](#) for $\delta^{18}\text{O}$ and $\delta^{13}\text{C}$. Isotope values are reported with a 1 σ precision of ± 0.03 for $\delta^{13}\text{C}$ and ± 0.06 for $\delta^{18}\text{O}$. Equilibrium calcite-water [fractionation](#) temperatures were calculated using the equation of [Friedman and O'Neil \(1977\)](#).

2.2. Geochemical modeling

Geochemical models were completed using GeoT version 2.1 ([Spycher et al., 2014](#)) and the associated tk-slt.h06_jun16.dat database ([Reed and Palandri, 2006](#)), coupled with the parameter optimization software iTOUGH2 ([Finsterle and Zhang, 2011](#)) using the PEST protocol ([Doherty, 2008](#); [Finsterle and Zhang, 2011](#)). The software and methods are described in detail by [Spycher et al. \(2014\)](#). GeoT coupled with iTOUGH2 ([Spycher et al., 2016](#)) automates the identification of processes described by [Reed and Spycher \(1984\)](#) that influence the clustering of mineral saturation indices about a given equilibration temperature (e.g. dilution, degassing, mixing). This method (optimized multicomponent solute geothermometry) has previously been applied to studies of various geothermal waters (e.g. [Battistel et al., 2014](#); [Peiffer et al., 2014](#); [King et al., 2016](#)).

3. Results

Fluid major and [trace element](#) results are presented in [Table 2](#) and [Fig. 6A](#) through D. [REE](#) results are presented in [Table 3](#) and [Fig. 7](#). Fluid δD and $\delta^{18}\text{O}$ values are presented in [Table 4](#) and [Fig. 10](#). $\delta^{13}\text{C}$ and $\delta^{18}\text{O}$ isotope measurements of [calcite](#) and equilibrium temperature calculations are presented in [Table 5](#).

Table 2. Major and [trace element](#) analytical results for Surprise Valley hot spring fluids.

	Units	SVHS Well	Seyferth's HS	Leonard's HS (BLM)	LCMV	CEC Exploratory Drill Hole	Spring E of SVHS (northern)	Spring E of SVHS (southern)	Spring SV of SVHS
Sample ID		20150824-1	20150825-1	20150825-3	20150825-4	20161101-1	20150824-2	20150824-3	20150824-4
Temperature	°C	97	83	69	99	~50	91	89	97
Conductivity (field)	mS	1.372	1.690	1.320	1.721	–	1.432	1.390	1.404
Conductivity (Lab)	mS	–	–	–	–	–	1.390	1.380	1.380
pH (field)	pH	8.46	7.81	8.29	7.47	–	8.29	8.20	8.17

	Units	SVHS Well	Seyferth's HS	Leonard's HS (BLM)	LCMV	CEC Exploratory Drill Hole	Spring E of SVHS (northern)	Spring E of SVHS (southern)	Spring SW of SVHS
pH (lab)	pH	8.64	8.05	8.47	8.05	8.6	8.45	8.48	8.5
Major elements (ICP-MS)									
Si	mg/L	44.8	49.8	49.2	89.0	44.6	–	–	–
Na	mg/L	266	306	320	316	282	–	–	–
K	mg/L	5.2	8.9	8.3	16.2	5.4	–	–	–
Ca	mg/L	16.7	29.5	26.9	24.8	19.2	–	–	–
Mg	mg/L	0.03	0.20	0.54	0.36	0.12	–	–	–
Major elements (ICP-AES)									
Na (soluble)	mg/L	–	–	–	–	–	273.6	273.6	273.6
Ca (soluble)	mg/L	–	–	–	–	–	18.8	19.0	18.6
Mg (soluble)	mg/L	–	–	–	–	–	<	<	<
B (soluble)	mg/L	5.9	7.8	5.3	6.6	5.8	5.9	5.9	5.8
Anions (ICP-AES)									
Cl	mg/L	178	197	164	201	186	174	173	173
SO₄	mg/L	327	407	312	333	333	–	–	–
NO₃	mg/L	<	<	<	<	<	–	–	–
HCO₃	mg/L	36.6	67.1	42.7	164.7	48.8	–	–	–
CO₃	mg/L	9.0	<	3.0	<	9.0	–	–	–
Charge balance error	%	–0.8	–0.4	13.1	0.4	0.4	–	–	–
Trace elements (ICP-MS)									
Li	µg/L	85.1	140	127	251	90.8	–	–	–
Al	µg/L	51.7	3.9	<	12.4	163	–	–	–
P	µg/L	8.1	8.7	11.5	23.4	52.7	–	–	–
V	µg/L	0.39	0.49	0.22	0.26	0.89	–	–	–
Cr	µg/L	0.05	0.07	0.09	0.06	0.23	–	–	–
Mn	µg/L	0.6	7.9	94.9	69.1	110.4	–	–	–
Fe	µg/L	1.08	2.02	5.46	12.64	2682	–	–	–
Cu	µg/L	0.17	0.06	0.07	0.13	0.31	–	–	–
Zn	µg/L	1.10	0.16	14.44	0.24	82	–	–	–
As	µg/L	191	365	378	305	71	–	–	–

	Units	SVHS Well	Seyferth's HS	Leonard's HS (BLM)	LCMV	CEC Exploratory Drill Hole	Spring E of SVHS (northern)	Spring E of SVHS (southern)	Spring SV of SVHS
Se	µg/L	2.7	3.2	2.8	2.0	<	–	–	–
Rb	µg/L	18.8	35.4	26.9	78.7	21.0	–	–	–
Sr	µg/L	219	542	170	1162	155	–	–	–
Mo	µg/L	33.0	37.7	39.1	36.2	20.9	–	–	–
Cd	µg/L	0.05	0.05	0.05	0.03	0.02	–	–	–
Sb	µg/L	3.5	7.4	5.4	14.8	2.7	–	–	–
Cs	µg/L	9.4	20.2	14.6	61.4	11.8	–	–	–
Ba	µg/L	5.8	21.4	6.3	31.9	6.1	–	–	–
Pb	µg/L	<	<	0.102	<	2.3	–	–	–
U	µg/L	<	<	<	<	0.01	–	–	–

Na, Ca and Si exceeded the calibration range at 1× dilution, thus, values are reported for analyses made on samples that were diluted 40× and adjusted accordingly.

The limit of detection (LOD) is $3\sigma_B/a$, where 'σB' is the standard deviation of the replicate analyses of the ratio of the analyte counts per second (CPS) to the internal standard (IS) CPS found in the calibration blank, and 'a' is the coefficient from the IS corrected calibration curve's regression equation:

$$y = ax + \text{blank.}$$

% Recovery is the average ($n = 5$) percent recovery of a 100 ppb standard solution (1000 ppb for B, Na, Mn, Al, Si, P, K, and Ca).

–Not analyzed.

<Less than the specified LOD.

Table 3. [Rare earth element](#) results.

Units	SVHS Well	Seyferth HS	Seyferth HS	Seyferth HS	LCMV	LCMV	NASS-6 seawater	LO D
	20150824-1 (F)	20150825-1 (F)	20150825-1 (F-DUP)	20150825-1 (U)	20150825-4 (F)	20150825-4 (F-DUP)		
Y	<	<	<	<	7.9	7.8	18.3	2.4
La	2.1	2.5	2.3	2.0	7.3	7.0	10.4	1.4
Ce	3.5	3.9	3.8	3.4	13.6	13.2	4.0	0.6
Pr	0.27	0.30	0.29	0.28	1.26	1.22	1.3	0.2
Nd	<	<	<	<	3.9	4.0	5.7	0.8
Sm	0.36	<	<	<	0.84	0.84	1.0	0.2

Units	SVHS Well	Seyferth HS	Seyferth HS	Seyferth HS	LCMV	LCMV	NASS-6 seawater	LO D
	20150824-1 (F)	20150825-1 (F)	20150825-1 (F-DUP)	20150825-1 (U)	20150825-4 (F)	20150825-4 (F-DUP)		
Eu	<	<	<	<	<	<	0.21	0.04
Gd	<	<	<	<	1.2	1.1	1.3	0.3
Tb	<	<	<	<	0.16	0.16	0.2	0.02
Dy	<	<	<	<	0.9	0.9	1.4	0.2
Ho	<	<	<	<	0.2	0.2	0.4	0.1
Er	<	<	<	<	0.6	0.6	1.2	0.2
Tm	–	–	–	–	–	–	–	–
Yb	<	<	<	<	0.5	0.5	1.1	0.1
Lu	<	<	<	<	0.08	0.08	0.2	0.02
% Tm spike recovery	98	98	99	92	93	92	95–107	–

Values in parts per trillion (picogram/kg).

(F) Filtered.

(U) Unfiltered.

(DUP) Duplicate sample run independently through entire preconcentration method.

% Recovery based on a 5 ppb TM spike.

LOD limit of detection.

LOD = 3.143 (Student's *t*-test value)*SD of *n* = 6 independently processed NASS-6 aliquots.

Table 4. [Stable isotope](#) (δD and $\delta^{18}O$) results for Surprise Valley hot spring fluids. Stable isotope measurements of some of these features have been made by other workers previously ([Reed, 1975](#); [Ingraham and Taylor, 1986](#); [Mariner et al., 1993](#); [Sladek et al., 2004](#)).

Sample ID	Site name	δD (VSMOW)	$\delta^{18}O$ (VSMOW)
20150824-1	Surprise Valley Hot Springs Well (SVHS)	-119	-14.3
20150824-2	Spring S of SVHS (northern)	-118	-14.2
20150824-3	Spring S of SVHS (southern)	-117	-14.2
20150824-4	Spring NW of SVHS	-119	-14.4

Sample ID	Site name	δD (VSMOW)	$\delta^{18}O$ (VSMOW)
20150824-5	Cold water well at Dessert Rose	-115	-14.9
20150824-6	Spring X	-120	-14.6
20150825-1	Seyferth/Chicken Hot Spring	-120	-14.2
20150825-2	Leonards Hot Spring East	-119	-14.1
20150825-3	Leonards Hot Spring West (BLM)	-117	-14.2
20150825-4	Lake City Mud Volcano (LCMV)	-114	-13.5
20160321-1	SVHS Hot Well	-117	-14.2
20160321-2	SVHS Reed Spring	-116	-13.5
20160321-3	Spring SW of SVHS	-119	-14.3
20160321-4	SVHS Flat Shack Spring	-118	-14.2
20160321-5	Spring E of SVHS (Small)	-117	-14.0
20160321-6	Spring E of SVHS (Northern)	-118	-14.2
20160321-7	Spring E of SVHS (Tiny)	-118	-13.8
20160321-8	Spring E of SVHS (Southern)	-118	-14.2
20160321-9	SVHS Cold Well	-113	-14.7
20160321-10	SVHS Hot Wellhead Near Ponds	-118	-14.4
	Drill Hole	-116	-14.0
Laboratory standard			
	Known value	-55.7	-8.04
	Mean (n = 11)	-55.3	-7.80
	1 SD	0.9	0.11

H₂O stable isotope analysis by laser spectroscopy (Los Gatos Research Instruments).

University of California-Davis Stable Isotope Facility.

Table 5. [Stable isotope](#) ($\delta^{13}C$ and $\delta^{18}O$) results for carbonate blocks ejected during the 1951 Lake City [Mud Volcano](#) Eruption, and carbonate from an adjacent fossil hot spring deposit.

Sample ID	$\delta^{18}O$ VSMOW	$\delta^{13}C$ PDB	Δ Temp. °C	
LCMV3- MC	0.99	-5.11	126	Multiple generations of bladed calcite
LCMV3- WR	1.33	-5.19	122	Carbonate mud on one side of bladed calcite sample
LCMV6- GB	3.04	-4.24	104	Bladed calcite away from Qz, Chl, Ad, and Py mineralization
LCMV6- BB	1.92	-4.38	115	Bladed calcite adjacent to minor Qz, Chl, Ad, and Py

Sample ID	$\delta^{18}\text{O}$ VSMOW	$\delta^{13}\text{C}$ PDB	^a Temp. °C	
LCMV7	7.04	-3.40	71	Actively forming travertine from a small pool with abundant organic matter
LCMV8F-B	1.44	-4.97	121	Honeycomb network of rhombic and bladed calcite veins surrounding voids - fine vein
LCMV8F-V	0.82	-5.30	128	Honeycomb network of rhombic and bladed calcite veins surrounding voids - large vein
LCMV8F-H	0.83	-5.03	127	Honeycomb network of rhombic and bladed calcite veins surrounding voids - fine lamination
LCMV9-O	5.18	-4.74	85	Vein composed of interlocking dogtooth calcite
FHS-1	4.43	-3.27	91	Fossil hot spring deposit with multiple generations of dogtooth calcite
FHS-2F	1.33	-5.43	122	Fossil hot spring deposit with rhombic calcite, clays and biogenic material
FHS-3F-MC	5.25	-3.40	85	Rhombic calcite, siliceous microbialites on one side of sample
FHS-3F-B	12.78	-2.08	35	Rhombic calcite, siliceous microbialites on one side of sample
FHS-3F-B	12.88	-1.93	35	Rhombic calcite, siliceous microbialites on one side of sample

Qz = [quartz](#); Chl = [chlorite](#); Ad = [adularia](#); Py = [pyrite](#).

a

Equilibrium temperature for calcite-water fractionation ([O'Neil et al., 1969](#)) using the $\delta^{18}\text{O}$ value measured for the LCMV hot spring water.

Fluid major element and [stable isotope](#) results are consistent with the results of previous studies (e.g. [Duffield and Fournier, 1974](#); [Reed, 1975](#); [Clawson et al., 1986](#); [Sladek et al., 2004](#)). LCMV fluids have lower pH, but elevated [bicarbonate](#), [silica](#), and [alkali](#) and [alkaline earth metals](#) (Li, K, Rb, Cs, Sr, and Ba) and REE, in both absolute concentrations and when normalized to a conservative element (e.g. Cl) compared to [thermal waters](#) from the eastern side of Surprise Valley ([Table 2](#), [Table 3](#); [Figs. 6A through D and 7](#)). Of the REE, only the light [rare earth elements](#) La, Ce and Pr (and Sm in SVHS) were detected in fluid samples from the eastern side of the Valley (Seyferth and SVHS). In contrast, only Eu was below the detection limit in the LCMV fluid sample from the western side of the valley ([Table 3](#)). Duplicate reproducibility for the LCMV sample was better than 5.5% for all REE, and 10% for the lower concentration Seyferth sample, except for La (16%). REE in an unfiltered sample from Seyferth hot spring had marginally lower values than the filtered and primary and

duplicate samples. The lower REE values in the unfiltered Seyferth sample are considered insignificant, as the difference is comparable to that between the primary and duplicate filtered samples. Eu was not detected in any of the samples, therefore quantification of an Eu anomaly is not possible. Qualitatively, there must be a negative Eu anomaly based on the magnitude of the Eu detection limits compared to the concentration magnitude of REE adjacent to Eu in the periodic table (Sm in the SVHS and Sm and Gd in the LCMV sample).

Hot spring fluids are shifted to heavier $\delta^{18}\text{O}$ values than local [meteoric water](#), and δD values span a range from local meteoric and groundwater (e.g. LCMV sample) up to 4.5‰ lighter (e.g. Seyferth HS) than the isotopically lightest groundwater (e.g. Desert Rose), and 3.1‰ lighter than the isotopically lightest snow measured by [Ingraham and Taylor \(1989\)](#) from Cedar Pass in the Warner Mountains ([Fig. 10](#); [Table 4](#)). [Oxygen isotope](#) equilibrium temperatures calculated for calcite blocks ejected from the LCMV eruption with bladed [crystal](#) forms range from 104 °C to 128 °C (mean 120 °C), assuming equilibrium with modern LCMV spring fluids ([Table 5](#)). Calcite with the lowest calculated equilibrium temperature (71 °C) was observed to be actively forming from a small LCMV thermal pool, and did not have a bladed crystal form. Equilibrium temperatures calculated for the fossil hot spring adjacent to the LCMV were all lower than 100 °C, again, assuming equilibrium with modern LCMV spring fluid. With one exception, calcite from the fossil hot springs had a rhombic or dogtooth crystal form. Calcite/water oxygen isotope equilibrium temperatures are approximations, and assume calcite formed from fluids with similar oxygen isotope values as modern LCMV fluids. Only limited historical data is available to evaluate if the [isotopic composition](#) of LCMV spring fluids have shifted over time. Hot springs with periodic and mild mud eruptions were present at LCMV prior to the 1951 [mud volcano](#) eruption, however, the temperature, chemistry and flow is relatively unknown as the main pools were in an area overgrown by tule ([White, 1955](#) and references therein). Following the 1951 LCMV eruption, geothermal features in the LCMV eruption crater include one boiling spring with weak geyser activity, at least two near-boiling springs, several small (<30 cm diameter) mudpots, and hot springs submerged by a small lake that fills part of the eruption crater ([Sladek et al., 2004](#)). [Reed \(1975\)](#) and [Sladek et al. \(2004\)](#) reported $\delta^{18}\text{O}$ values of -14.8 and -13.5‰ and δD values of -113 and -114‰, respectively, for boiling LCMV [spring waters](#), in good agreement with values measured in this study.

4. Discussion

4.1. Classical geothermometry results

Classical geothermometers ([Table 6](#)) applied to sample results in [Table 2](#) yield temperatures that span a wide range for each location, consistent with results from previous basin-wide studies (e.g. [Duffield and Fournier, 1974](#); [Reed, 1975](#); [Sladek et al., 2004](#)). Lack of agreement between classical [geothermometry](#) results listed on [Table 6](#) preclude directly inferring maximum fluid equilibration temperatures, however, the relationships between results are useful for informing more detailed geochemical models. In the following discussion, we initially focus on geothermometry results for LCMV fluids. Previous studies suggested that high conservative element (Cl, B) concentrations in LCMV spring fluids reflect an undiluted primary deep geothermal fluid in equilibrium with [quartz](#) at depth, an assumption that has provided the basis for many conceptual models of the Surprise Valley [geothermal system](#).

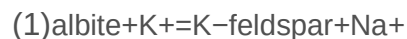
Table 6. Classical [geothermometry](#) calculations using results from [Table 2](#) and equations from the cited studies.

	SVHS Well	Seyferth HS	Leonard HS (BLM)	LCMV	Drill hole	Phipps-2corrected for steam loss (Sladek et al., 2004)
Measured temperature	97	83	69	99	~50	170
Quartz conductive (Fournier and Potter, 1982)	135	141	140	177	135	208
Chalcedony conductive (Fournier, 1977)	108	115	114	155	108	190
Alpha Cristobalite (Fournier, 1977)	84	90	90	127	84	158
Amorphous Silica (Fournier, 1977)	15	20	20	53	15	82
Na/K (Fournier, 1977)	108	130	123	166	107	202
Na/K (Giggenbach, 1988)	129	150	143	184	128	218
Na-K-Ca (Fournier and Truesdell, 1973)	92	100	100	155	91	194
K/Mg (Giggenbach, 1988)	129	114	98	123	107	Mg below detection
Li/Mg (Kharaka and Mariner, 1989)	110	95	80	103	90	Mg below detection

Quartz geothermometry results (assuming conductive cooling) predict LCMV fluids equilibrated at 177 °C ([Table 6](#)), a similar value to those obtained in previous studies and similar to the maximum bottom hole temperature of 170 °C measured in the Phipps-

2 well ([Rigby and Zebal, 1981](#)), but much lower than the geothermometry results calculated for deep thermal fluids from the Phipps-2 geothermal well of 208 °C ([Sladek et al., 2004](#); [Table 6](#)). The quartz geothermometer works best at temperatures above about 150 °C ([Fournier, 1977](#)). At lower temperatures, slow quartz precipitation kinetics leads to controls on dissolved [silica](#) concentrations by lower-order silica polymorphs (e.g. [chalcedony](#), [cristobalite](#), amorphous silica) or possibly by [silicate minerals](#) other than quartz. For example, silica is an important component of reactions (2) and (3), shown below. Silica geothermometers underestimate equilibration temperatures upon mixing with dilute waters, because calculated temperatures directly depend on the absolute silica concentration.

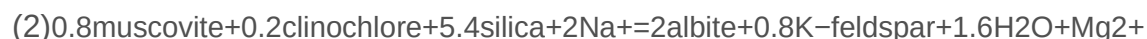
Na/K geothermometer results for the LCMV sample are within 11 °C of the quartz geothermometer value for the LCMV sample ([Table 6](#)), and span the maximum measured temperature of 170 °C in Phipps-2. The Na/K geothermometers closely approximate, or are based on [thermodynamic equilibrium](#) between [albite](#) and [potassium feldspar](#) ([Fournier, 1979](#); [Giggenbach, 1988](#)):



The kinetics of [reaction \(1\)](#) proceed slowly below about 180 °C. Thus, Na/K ratios are readily modified at lower temperatures during outflow by leaching of Na along flow paths and/or removal of K into [secondary minerals](#), particularly if flow rates are low ([Giggenbach, 1988](#)). This results in elevated Na/K ratios and lower calculated Na/K temperatures, a process possibly responsible for lower LCMV Na/K geothermometry results compared to deep geothermal water from the Phipps-2 well ([Table 6](#)).

Considering the maximum measured well and [borehole](#) temperatures of 160–170 °C, and very [low flow](#) rates for most LCMV hot springs as reported by [Sladek et al. \(2004\)](#), Na/K geothermometer results for Surprise Valley waters are not likely set by [reaction \(1\)](#), and close agreement with the classical quartz geothermometer is probably coincidental.

In contrast to the Na/K geothermometer, the kinetics of reactions that form the basis of the K/Mg geothermometer proceed rapidly, even below 100 °C ([Giggenbach, 1988](#)):



Comparing temperatures obtained using the [Giggenbach, 1988](#) Na/K and K/Mg geothermometers form the basis of the Na-K-Mg triangular 'Giggenbach' plot routinely used to evaluate the equilibrium state of geothermal waters. When temperatures calculated using Na/K and K/Mg geothermometers agree, waters are considered fully equilibrated ([Giggenbach, 1988](#)). The K/Mg geothermometer applied to the LCMV

sample yields a temperature of 123 °C, much lower than feldspar and quartz equilibrium would predict, suggesting possible fluid equilibration at lower temperatures. Mg is typically present at higher concentrations in dilute cold fluids than thermal fluids, so even small degrees of mixing can reduce calculated K/Mg temperatures. Likewise, dissolution of an Mg-rich [evaporite](#) mineral would lower K/Mg temperature estimates. On the other hand, if the K/Mg geothermometer accurately reflects the fluid equilibration temperature, then it is unlikely that silica concentrations are controlled by quartz solubility at these low temperatures. Controls on silica concentrations by minerals other than quartz at low temperatures are expressed in Eqs. [\(2\)](#), [\(3\)](#).

The empirical Na-K-Ca geothermometer was developed to accommodate shortcomings in the temperature limits of the Na/K geothermometer, and can provide a reliable indicator of last equilibration temperatures for fluids in the 4 to 340 °C temperature range ([Fournier and Truesdell, 1973](#)). The predicted Na-K-Ca equilibration temperature for LCMV (155 °C) is lower than that calculated for Phipps-2 (194 °C) ([Table 6](#)). [Calcite](#) precipitation and associated Ca-loss from fluids increases predicted Na-K-Ca temperatures, while mixing with dilute Ca-bearing waters tends to underestimate Na-K-Ca temperatures (c.f. [Fournier and Truesdell, 1973](#)). Calcite is known to precipitate in the subsurface of the LCMV area based on observations from drill cores ([Benoit et al., 2005b](#)), calcite blocks ejected from the 1951 LCMV eruption, and calcite observed to be actively forming (and sampled in this study) from one LCMV spring. Calcite precipitation would suggest that Na-K-Ca geothermometer results overestimate LCMV spring temperatures, however mixing with dilute Ca-bearing waters and modification of Na and K by equilibration at lower temperatures would counter this effect.

The Li-Mg geothermometer was developed to estimate subsurface temperatures in the 30 to 200 °C for sedimentary basin [formation waters](#), where fluid [salinities](#) and hydraulic pressures are typically higher than for convective geothermal systems ([Kharaka and Mariner, 1989](#)). In this study, the calculated Li-Mg temperature is lower than, but comparable to, results for the low-temperature K/Mg geothermometer but inconsistent with Na/K, Na/K/Ca, or quartz geothermometry results. The empirical Li-Mg geothermometer was calibrated using sedimentary formation water samples, thus, results applied to Surprise Valley should be viewed with some skepticism. Li-based geothermometers are also sensitive to processes including steam loss and dilution, which can lead to erroneous results ([Fouillac and Michard, 1981](#)). An additional problem is that Li is typically present at much lower concentrations than ions used in other geothermometer formulations, thus, analytical results are susceptible to higher relative

analytical error and measurement accuracy can negatively influence geothermometry results.

In summary, disagreement between results for different classical geothermometer formulations are consistent with modification of Surprise Valley hot spring fluids relative to deep geothermal fluids. Possible mechanisms include mixing with dilute waters (dilution) or low temperature equilibration (re-equilibration); models proposed previously to describe the relationship of fluids on the east side of the valley to the LCMV area (i.e. [Duffield and Fournier, 1974](#); [Sladek et al., 2004](#)). It is also possible that dissolution of Mg, K and Na-bearing evaporite minerals by hot spring fluids could influence [cation](#) geothermometer results, considering hot springs in Surprise Valley manifest in proximity to [alkali lake waters](#) that are predicted to form Mg, K and Na-bearing minerals upon evaporation ([Fowler et al., 2017](#)). Identifying the primary modification mechanism is essential for informing a conceptual model of the geothermal system, but is not possible using classical geothermometry techniques alone.

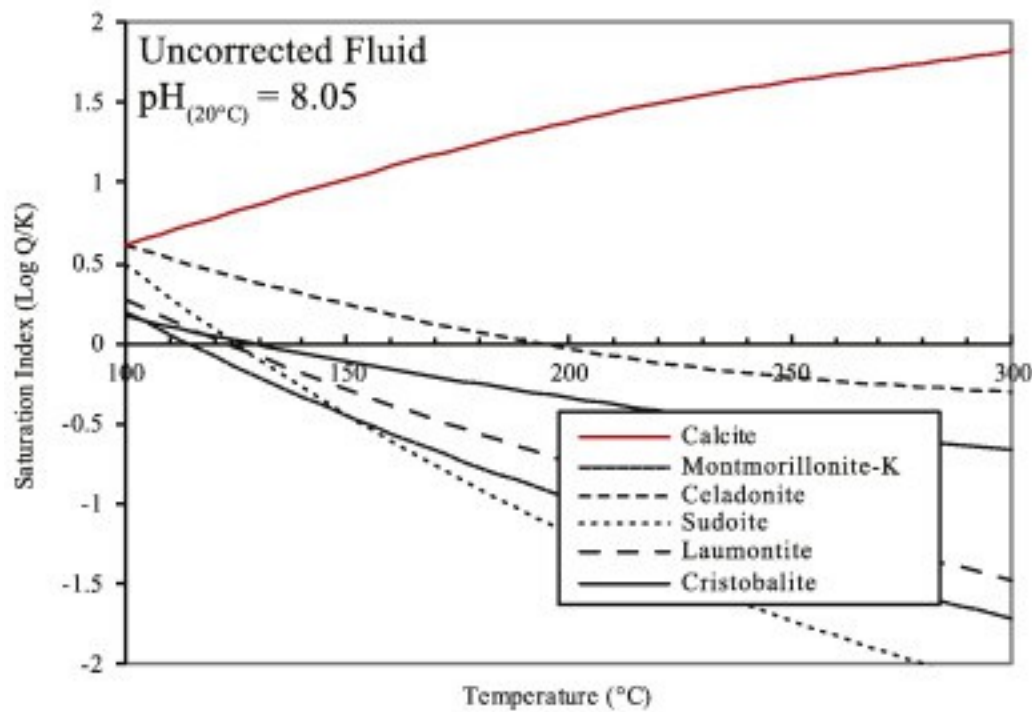
4.2. Multicomponent geothermometry modeling

We constructed multicomponent geothermometry models of measured spring fluid chemistries to test dilution and low temperature equilibration models. We completed models for samples analyzed from LCMV, SVHS, Seyferth, and Leonards hot springs. We did not model the sample from the [CEC](#) exploratory drillhole because the sample had no associated pH measurement and anomalously high Fe (as well as V, Cr, and Se), probably sourced from contamination by metal alloys in the [drill bit](#), grease on the drilling equipment, or [drilling fluids](#) ([Table 2](#)). Based on this observation, we didn't have sufficient confidence in results for other dissolved components to complete rigorous geochemical modeling on the sample. We note that many dissolved components in the CEC drillhole fluid sample are nearly identical to those in the fluid sample from the adjacent SVHS well ([Table 2](#)), so fluids in these two locations likely have a similar history.

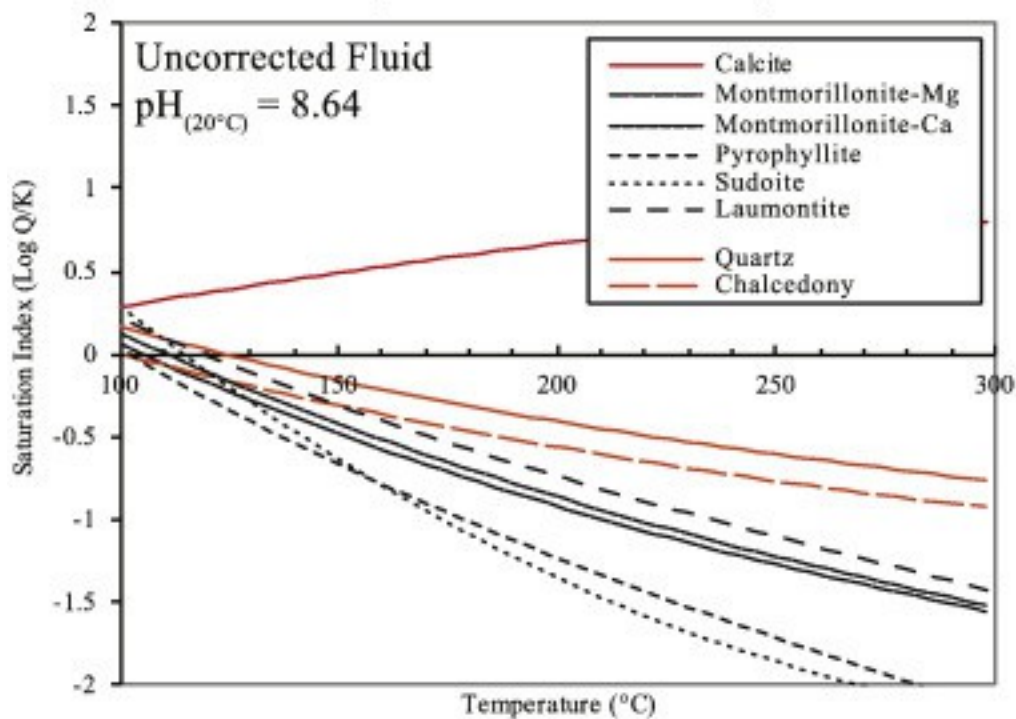
For our models, we utilized laboratory measurements of pH, Si, Na, K, Ca, Mg, Al, SO_4 , Cl, and HCO_3 . We modeled three scenarios for each sample. The first model was run in GeoT using only measured pH values and the chemical species listed above (uncorrected model; [Fig. 2A](#) through C). The second model explored mixing with infinitely dilute waters (dilution model; [Fig. 3A](#) through C), and the third model explored low temperature re-equilibration of spring fluids (re-equilibration model; [Fig. 4A](#) through D). In the dilution and reequilibration models, we accounted for the effect of CO_2 -bearing vapor loss from boiling. This approach is supported by observations of bladed calcite in

LCMV calcite blocks and veins in OH-1 and LCSH-5 drill cores, a calcite morphology associated with CO₂ flux ([Simmons and Christenson, 1994](#)). Bladed calcite is usually associated with boiling, which would result in [gas phase](#) separation ([Browne, 1978](#)). Field observations of weak but active bubbling in several Surprise Valley hot springs was also observed during sampling. To account for CO₂ loss on boiling in the models, we assumed the vapor contained 99.9% H₂O and 0.1% CO₂, and used [parameter estimation](#)(PEST; [Finsterle and Zhang, 2011](#)) coupled with the steam water fraction (stwf) input option in GeoT to calculate the ideal fraction of this hypothetical vapor that would be compatible with assumed mineral assemblage. Al was below detection in the sample from Leonards spring, so we optimized both the stwf and Al concentration in this sample.

LCMV Multicomponent Geothermometry Calculations



SVHS Multicomponent Geothermometry Calculations

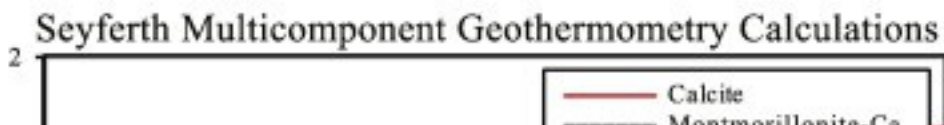
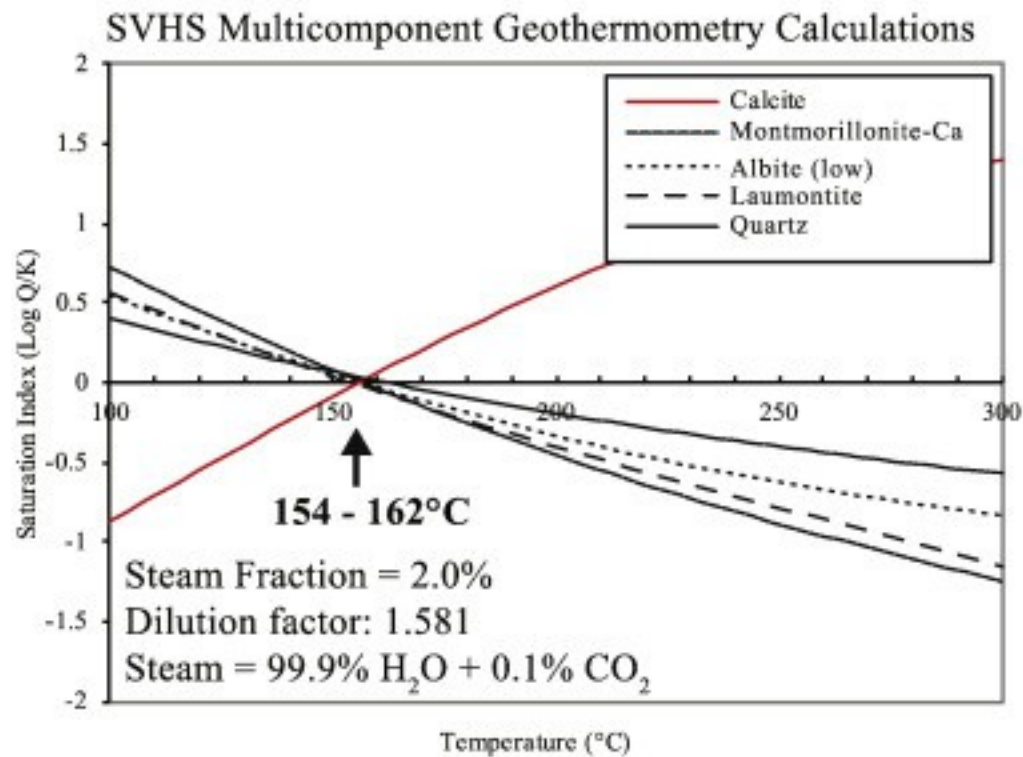
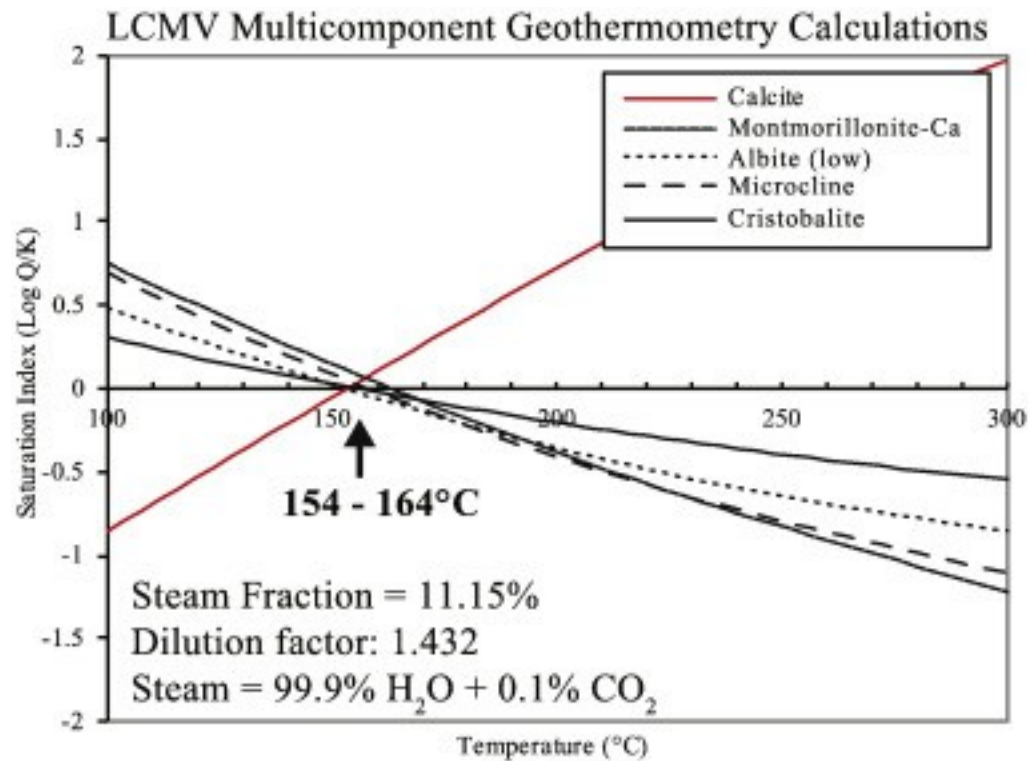


Seyferth Multicomponent Geothermometry Calculations



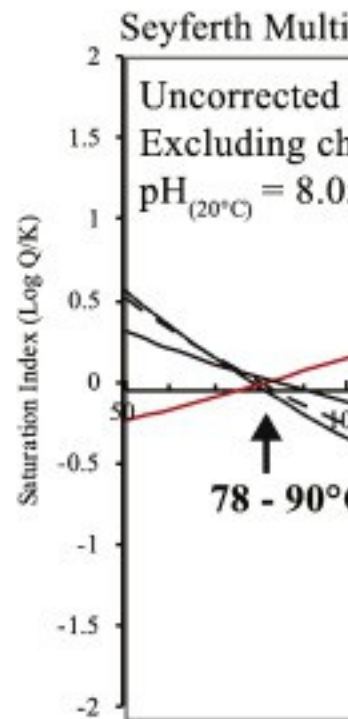
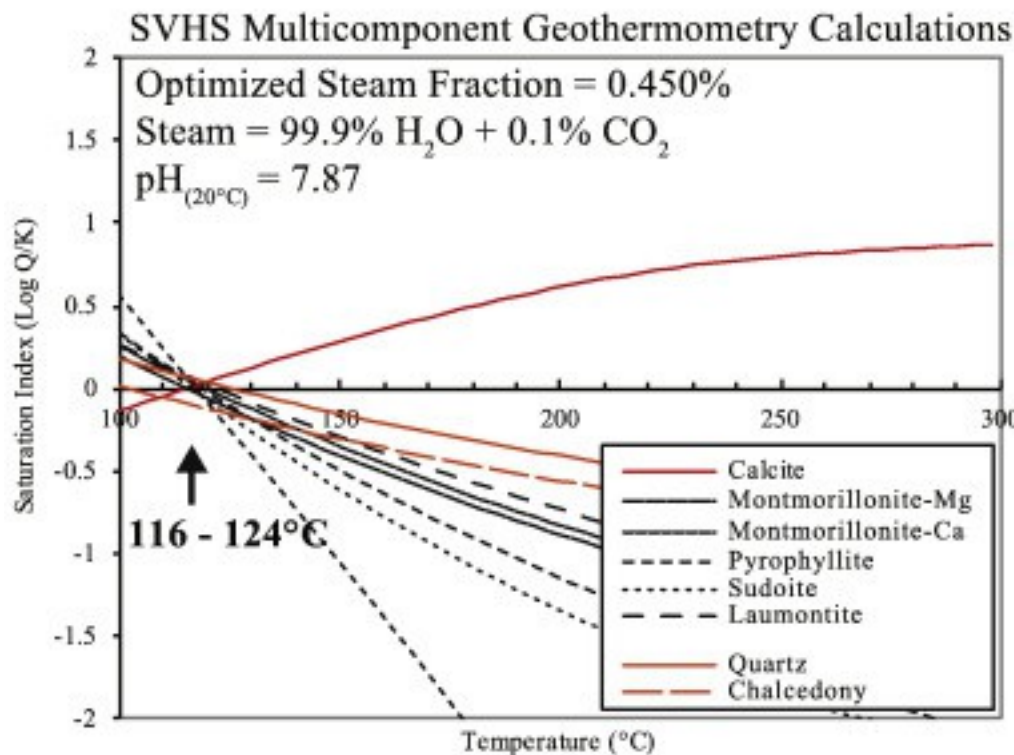
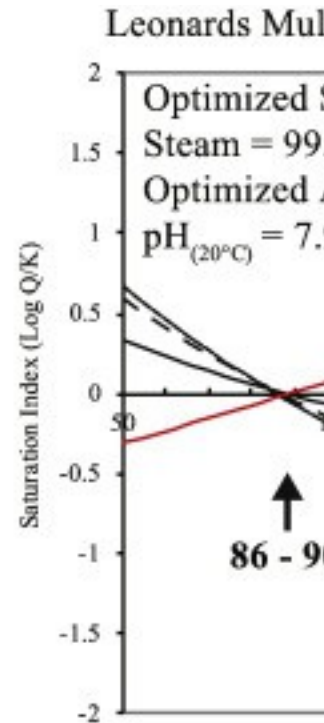
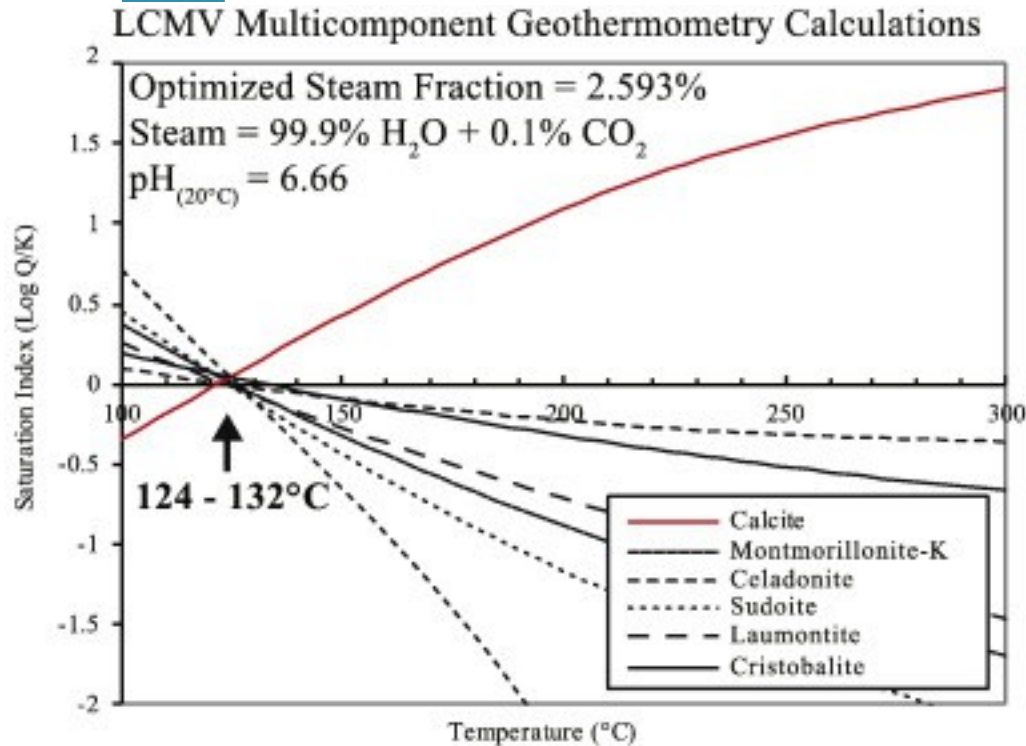
1. [Download high-res image \(752KB\)](#)
2. [Download full-size image](#)

Fig. 2. A through C: Mineral saturation indices computed using GeoT with uncorrected (as-is) fluid analyses listed in [Table 2](#).



1. [Download high-res image \(752KB\)](#)
2. [Download full-size image](#)

Fig. 3. A through C: Mineral saturation indices computed using GeoT with fluid analyses listed in [Table 2](#) but corrected to account for dilution.



1. [Download high-res image \(1MB\)](#)
2. [Download full-size image](#)

Fig. 4. A through D: Mineral saturation indices computed using GeoT with fluid samples listed in [Table 2](#) and low-temperature equilibration minerals. LCMV and SVHS mineral saturation indices corrected for CO₂ loss, Seyferth and Leonards spring results as-is. We constrained [mineralogy](#) in the three model scenarios using secondary minerals identified in an extensive study of altered rocks drilled from holes OH-1 and LCSH-5 by [Moore and Segall \(2005\)](#). Holes OH-1 and LCSH-5 were drilled nearby to Phipps-2 in 2002, and both wells achieved maximum temperatures of approximately 160 °C during testing, comparable to the bottom hole temperature measured in Phipps-2 ([Benoit et al., 2005b](#)). Two main stages of secondary mineralization were identified in these rocks: 1) a clay (smectite and chlorite), quartz, [zeolite](#), and calcite assemblage, and 2) a later stage of silica as quartz, chalcedony, or possibly amorphous silica deposition ([Benoit et al., 2005b](#); [Moore and Segall, 2005](#)).

In the uncorrected models, calcite is supersaturated in surface [spring waters](#), consistent with the observation of calcite actively precipitating from an LCMV spring ([Table 5](#)), but saturation indices do not cluster about a given temperature for other minerals in the models for LCMV and SVHS ([Fig. 2A](#) and [B](#)). The uncorrected model for Seyferth spring resulted in clustering of mineral saturation indices at the measured spring temperature, except for sudoite and [celadonite](#).

Mineralogy in the dilution models were constrained using minerals identified near the base (934 to 4565 m) of holes OH-1 and LCSH-5, where calcite and quartz [fluid inclusion](#) temperatures range from 132 °C to 183 °C ([Moore and Segall, 2005](#)). Clay-sized minerals identified in this depth range include calcite, [laumontite](#), silica (quartz, cristobalite and amorphous silica), trace [smectite](#), and unidentified feldspar. The following minerals were selected from the GeoT database to represent the observed mineralogy in the dilution models: calcite, laumontite, cristobalite, quartz, beidellite-Na and montmorillonite-Ca (smectite group), albite and [microcline](#) (feldspar group). In addition, we found that [anhydrite](#) and [pyrophyllite](#) equilibration temperatures were compatible with the dilution models, however these secondary minerals have not been reported in Surprise Valley rocks to our knowledge, and are, thus, excluded from the models.

In the dilution models, CO₂-bearing steam loss of 0.3 to 12.4% coupled with concentration factors of ~1.5 are required for saturation indices of the selected mineral assemblage to cluster about a given temperature ([Fig. 3A](#) through [C](#)). The resulting equilibration temperatures range from 140 to 166 °C for LCMV, SVHS and Seyferth,

comparable to measured temperatures in geothermal wells and exploration boreholes. While the dilution model temperatures and dilution factors of about 1.5 are very similar for the LCMV and SVHS samples, the mineral assemblages and fractions of steam loss differ. Cristobalite is included in the LCMV sample while quartz is included in the SVHS assemblage, and the LCMV sample requires correction for a steam fraction of 11.2 %, while the SVHS sample requires only 2 %.

The re-equilibration models were constrained using the mineralogy of an active feed zone identified in well OH-1 at a depth of 288.6 m and a measured (sub-boiling) temperature of 133 °C. The temperature of this zone is close to the maximum calcite-fluid [oxygen isotope fractionation](#) temperature of 128 °C calculated for blocks ejected from the LCMV eruption ([Table 4](#)). The temperature similarity is perhaps coincidental, considering the calcite blocks may not have formed from modern subsurface temperature conditions and the only age constraint is pre-1951, the year the [mud volcano](#) erupted. Mineralization associated with the feed zone and core samples within 4 to 60 m of the feed zone include: Mg-rich [chlorite](#), celadonite, and botryoidal silica initially deposited as a silica polymorph other than quartz, trace smectite, laumontite, and calcite ([Moore and Segall, 2005](#)). The following minerals were selected from the GeoT database for the re-equilibration model: calcite (CaCO_3), celadonite ($\text{KMgAlSi}_4\text{O}_{10}(\text{OH})_2$), laumontite ($\text{Ca}(\text{AlSi}_2\text{O}_6)_2 \cdot 4\text{H}_2\text{O}$), cristobalite (SiO_2), montmorillonite-K (smectite group; $\text{K}_{0.33}\text{AlMg}_2\text{Si}_4\text{O}_{10}(\text{OH})_2$), and sudoite (Mg-chlorite; $\text{Mg}_2\text{Al}_3(\text{Si}_3\text{Al})\text{O}_{10}(\text{OH})_8$). Thus, the re-equilibration model differed from the dilution model in that albite, microcline and quartz were excluded, minerals that are not stable at low temperatures. Several options for cristobalite are available in the GeoT database, including b-cristobalite and cristobalite. We chose not to use b-cristobalite, as data for this phase was originally sourced from experiments performed on a natural [sinter](#) from Yellowstone National Park that was not true cristobalite but more likely opal-cristobalite.

The GeoT-iTOUGH2 simulation for CO_2 -bearing vapor loss results in clustering of the mineral saturation indices around 124–132 °C for the LCMV sample, if 2.6% loss of the modeled vapor is accounted for ([Fig. 4A](#)). We attempted this model using different values for the CO_2 ratio in steam, and this resulted in slight variations in the calculated steam fraction, but little difference in the calculated equilibrium temperature. Thus, pH changes associated with CO_2 correction rather than the H_2O fraction (i.e. dilution) is the variable influencing mineral solubility and clustering of saturation indices. For SVHS, a minor steam fraction correction (0.1%) resulted in convergence of the mineral assemblage between 116 and 124 °C ([Fig. 4B](#)). Both quartz and chalcedony saturation indices are in close agreement with, but span, the estimated equilibration temperature.

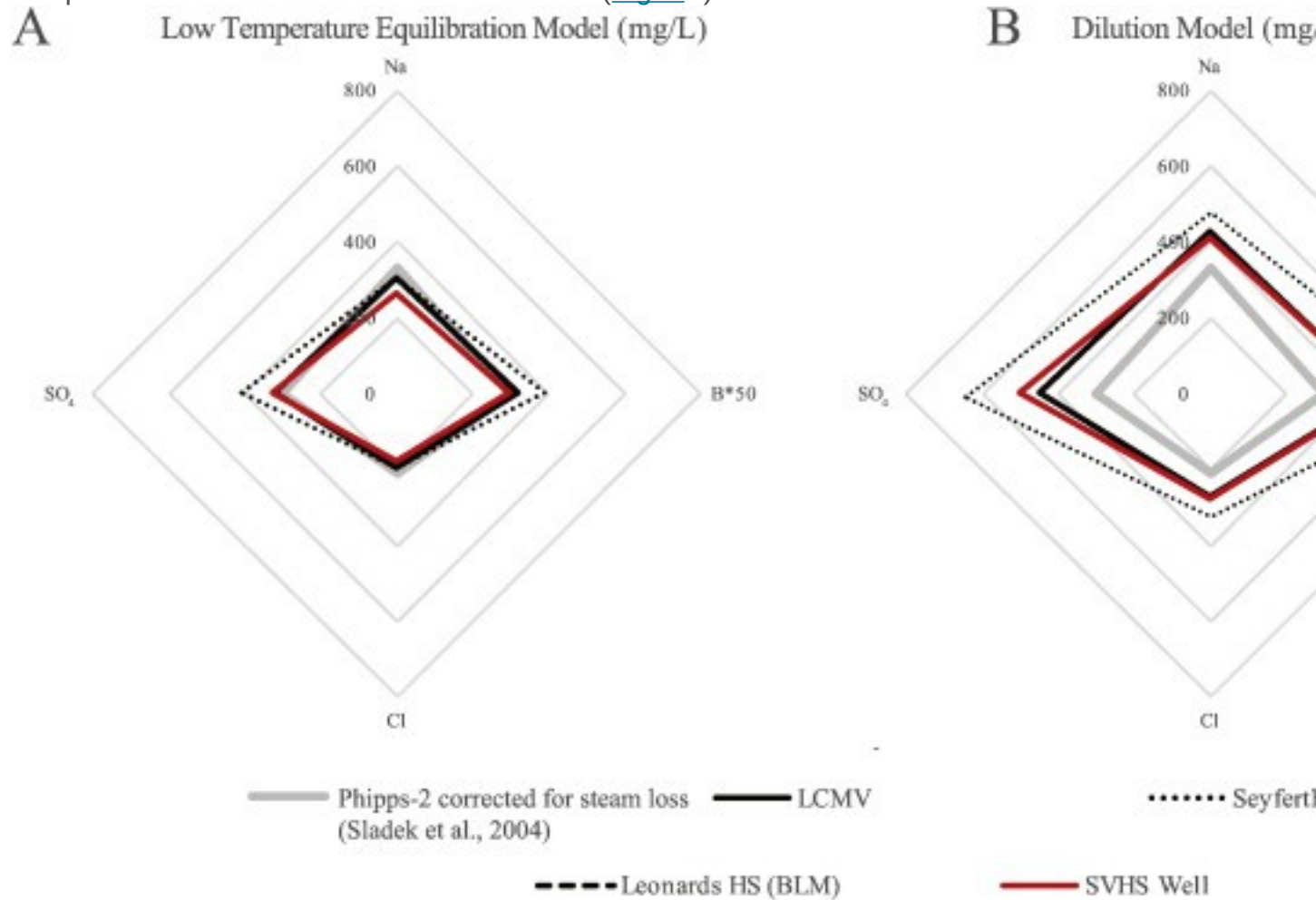
Quartz and chalcedony were not included in the optimization calculation because these silica polymorphs are usually kinetically controlled at low temperatures and therefore may not control silica concentrations at the model temperature. For Seyferth spring, the lack of sudoite and celadonite equilibrium at the measured spring temperature can be reconciled if the lower limit of formation for these minerals is assumed to be over 100 °C. If sudoite and celadonite are excluded from the model for this reason, the saturation indices for the remaining minerals cluster around 78–90 °C compared to the measured temperature of 83 °C ([Fig. 4C](#)). No CO₂ loss correction is required, suggesting spring waters are in equilibrium with the measured spring temperature. A similar result was obtained for Leonards spring ([Fig. 4D](#)).

In summary, the multicomponent geothermometry models yield plausible results for both dilution and low-temperature equilibration models. The multicomponent geothermometry models have the benefit over classical geothermometry methods in that they readily provide numerical values for a variety of conditions (e.g. steam loss, dilution factors, CO₂ loss) required to achieve equilibrium with a selected mineral assemblage. These results provide a basis to further evaluate the plausibility of each fluid evolution scenario. It is emphasized that the models are subject to the underlying assumption of equilibrium and limitations of the [thermodynamic](#) data used (see [Spycher et al., 2014](#) for discussion).

4.3. Reconciling dilution and re-equilibration models: dissolved major and trace element data

Mineral saturation indices in the dilution models cluster about higher temperatures (122 to 166 °C; [Fig. 3A–C](#)) than in the re-equilibration models (78 to 132 °C; [Fig. 4A–D](#)). For mineral saturation indices to cluster about a given temperature, the dilution models require a greater steam loss fraction than in the re-equilibration models (up to 11.15% for LCMV), in addition to high concentration factors (around 1.5) to correct for dilution. [Fig. 5A](#) and [B](#) graphically show the results of correcting hot spring major and [trace element](#) concentrations for the steam loss and dilution factors in the computed GeoT re-equilibration and dilution models. The steam loss correction is very small in the GeoT re-equilibration models, thus, the results shown in [Fig. 5A](#) are almost indistinguishable from the measured concentrations shown in [Fig. 6A](#). Absolute and relative concentrations of Na, B, Cl, and SO₄ are very similar in all hot springs and compared to the steam-loss corrected deep geothermal fluid from Phipps-2 in the re-equilibration models ([Fig. 5A](#)). For the dilution models, Na, B, Cl, and SO₄ concentrations in the LCMV, SVHS, and Seyferth samples are higher than in the

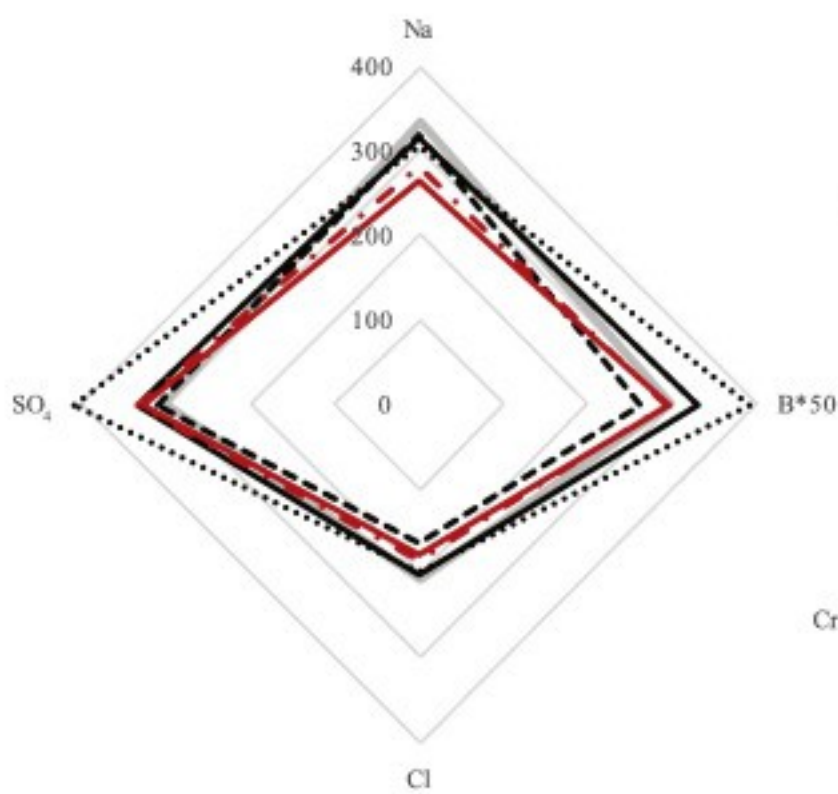
steam-loss corrected Phipps-2 sample after correction for dilution using the respective computed concentration factors of around 1.5 (Fig. 5B).



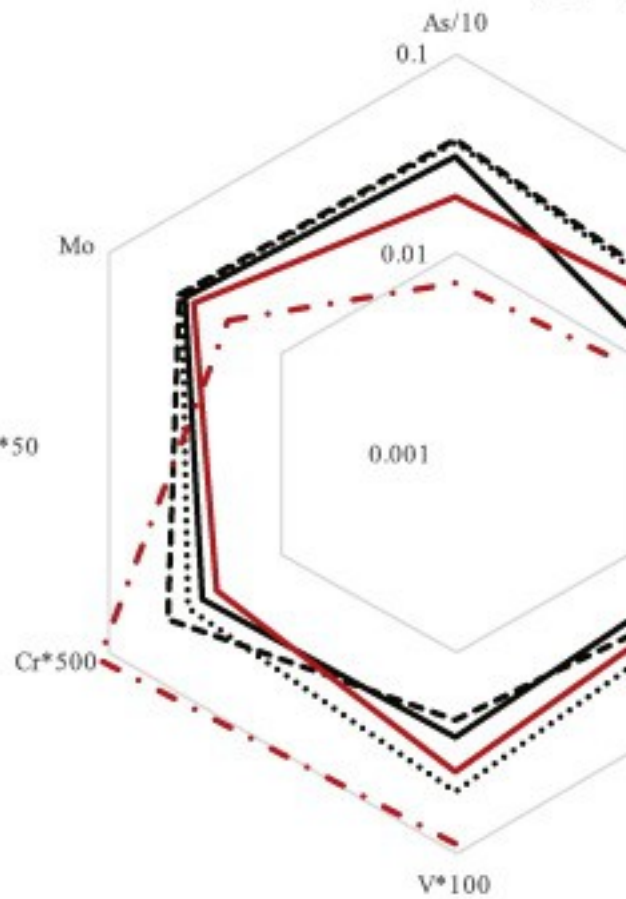
1. [Download high-res image \(352KB\)](#)
2. [Download full-size image](#)

Fig. 5. Graphical relationships of conservative element concentrations in the steam loss-corrected sample from Phipps-2 (Sladek et al., 2004) compared to computed concentrations in Surprise Valley hot spring waters, assuming: A) re-equilibration and B) dilution.

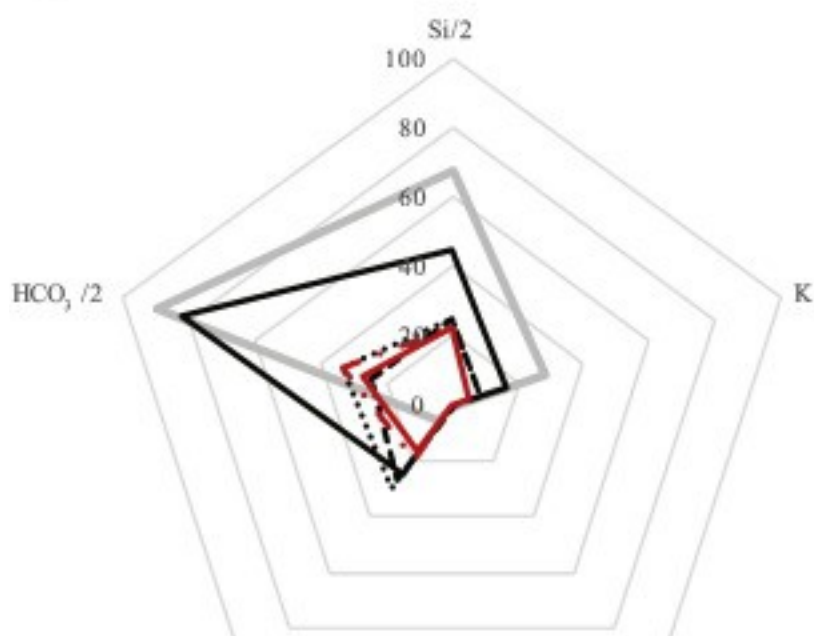
A Major Elements (mg/L)



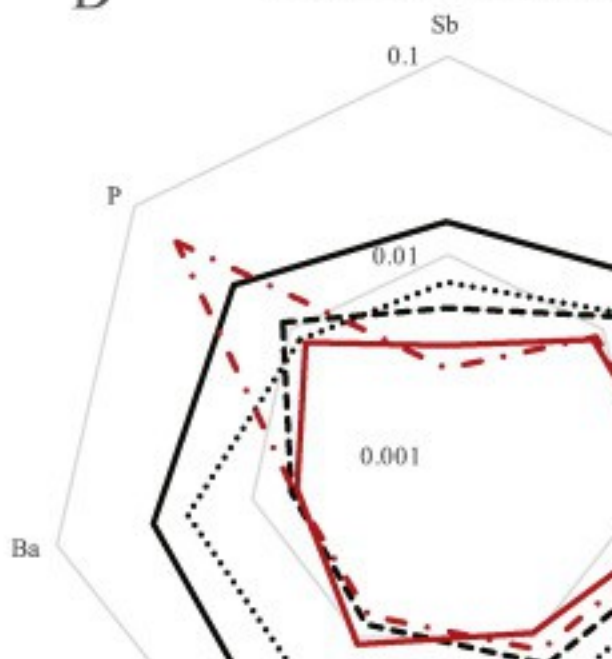
B Trace Elements (ug/L)



C Major Elements (mg/L)



D Trace Elements (ug/L)



1. [Download high-res image \(856KB\)](#)
2. [Download full-size image](#)

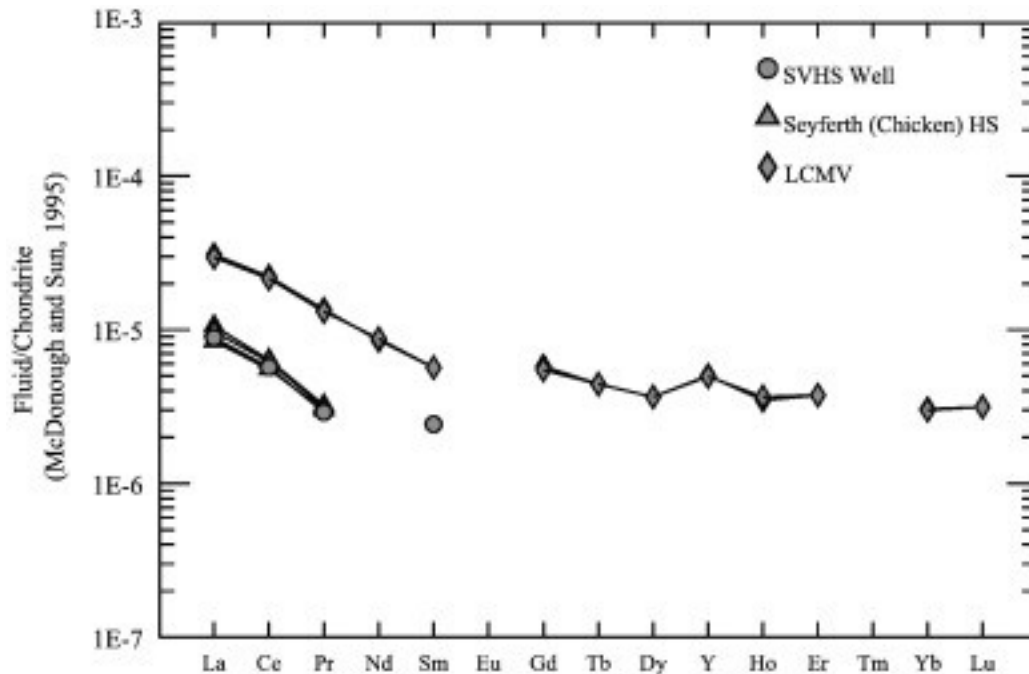
Fig. 6. A through D: Graphical relationships of major element concentrations in Surprise Valley hot spring waters compared to the steam loss-corrected sample from Phipps-2 ([Sladek et al., 2004](#)). Note that panels B and D are displayed on a logarithmic scale, and [trace element](#) data shown in panels B and D are unavailable for the Phipps-2 sample.

[Fowler et al. \(2015\)](#) modeled the [Sladek et al. \(2004\)](#) Phipps-2 well sample (reconstructed for steam loss) using GeoT, and showed that dilution was not required for the fluid to be in equilibrium with a reasonable mineral assemblage at 228 °C, when the reported steam loss fraction and CO₂ degassing were accounted for. Results of various classical geothermometers applied to the steam loss-corrected Phipps-2 sample suggest equilibration temperatures of 194 to 218 °C ([Table 6](#)), in accordance with dissolved sulfate oxygen isotope temperature estimates for hot springs on the eastern side of the valley, which range from 200 °C to 208 °C ([Reed, 1975](#); [Nehring et al., 1979](#)). The higher temperatures predicted by these various methods suggest the Phipps-2 sample is the best available example of an undiluted endmember geothermal fluid in Surprise Valley. As such, corrections for processes including steam loss and dilution should yield element concentrations that approach those in the reconstructed Phipps-2 sample. The Na, B, Cl, and SO₄ concentrations in the LCMV, SVHS and Seyferth samples, after correction for computed concentration factors in the GeoT dilution models, significantly exceed steam-loss corrected values of the same components in the geothermal fluid from the Phipps-2 well ([Fig. 5B](#)). This result suggests that the high computed concentration factors required for hot spring samples to be in equilibrium with a mineral assemblage at elevated temperatures are unrealistic.

If dilution is discounted and the measured [fluid compositions](#) (uncorrected for dilution) are instead examined, the major dissolved components and trace element concentrations broadly fall into two groups. One group has absolute and relative concentrations comparable in all hot spring samples ([Fig. 6A](#) and B), while the other group has systematic variations in absolute concentration between different hot springs ([Fig. 6C](#) and D). The major dissolved components Na, B, Cl, and SO₄ have similar concentrations in all hot springs, aside from slightly elevated B and SO₄ in the Seyferth sample ([Fig. 6A](#)). The same is largely true of As, Cd, Se, V, Cr and Mo ([Fig. 6B](#)). The second group of dissolved components, which include Si, HCO₃⁻, and K, consistently have the highest concentrations in Phipps-2, intermediate concentrations in the LCMV sample, and lower concentrations in samples from Seyferth, Leonards, SVHS and the

CEC borehole from the eastern side of the valley ([Fig. 6C](#)). Ca concentrations follow the inverse of this pattern. Trace element data are not available for the Phipps-2 sample, but alkali and alkaline earth elements (Li, Rb, Cs, Sr, and Ba), along with P, Sb, and Fe, also generally follow the same pattern of highest concentrations the LCMV spring to lowest in springs on the eastern side of the valley ([Fig. 6D](#) and [Table 2](#)). The CEC drillhole water sample proves an exception to this general grouping of elements, and has elevated Cr, V, Fe, P and lower Mo, As, Cd and Se relative to surface hot springs ([Fig. 6B, D](#) and [Table 2](#)). The elements with elevated concentrations in the CEC sample are potentially sourced from Fe-alloys in drilling equipment, drilling mud/grease, or host rocks/sediments that were disturbed during drilling.

[Rare earth elements](#) also fall into the second group of elements; LCMV fluids have higher absolute concentrations but similar [chondrite](#) normalized patterns to SVHS and Seyferth spring on the east side of the valley ([Fig. 7](#); [Table 3](#)). Dilution factors ranging from 2.3 to 5 would be required to produce the measured [REE](#) in the SVHS and Seyferth samples from the LCMV sample. The magnitude of the REE-based dilution factors and required dilution relationship between different springs is inconsistent with the concentration factors computed in the GeoT dilution models (i.e. [Fig. 3A](#) through C). Rather than dilution, mineral precipitation and [sorption](#) of REE onto [mineral surfaces](#) may control dissolved REE concentrations. REE are strongly partitioned into carbonate compared to geothermal fluids (see review by [Debruyne et al., 2016](#)), therefore carbonate precipitation provides one mechanism to remove REE from fluid. Fluid REE concentrations are also controlled by sorption onto clay mineral surfaces, Fe-oxides and carbonates ([Coppin et al., 2002](#); [Quinn et al., 2006](#)), and this effect is increased as temperature decreases ([Bau, 1991](#)). Thus, partitioning of REE into secondary minerals formed during low temperature re-equilibration, or sorption onto mineral surfaces present along an eastward flow path, could explain lower REE concentrations in Seyferth and SVHS fluids on the eastern side of the valley compared to LCMV.



1. [Download high-res image \(127KB\)](#)
2. [Download full-size image](#)

Fig. 7. Chondrite normalized rare earth element concentrations of Surprise Valley hot spring fluids.

Modification of spring concentrations through dilution by relatively pure water is also inconsistent with the fluid major and trace element characteristics. The group of elements with generally similar concentrations includes elements that behave conservatively through mixing and dilution (e.g. Cl, B). Dilution at different concentration factors should result in different conservative element concentrations between hot springs. On the other hand, equilibration of fluids at progressively lower temperatures would maintain consistent conservative element ratios, but deplete fluids in more reactive elements. If hot spring fluids originated with a composition similar to the reconstructed Phipps-2 well sample, elements undersaturated with respect to minerals that would remove them from solution during re-equilibration at progressively lower temperatures would behave conservatively. Elements incorporated into secondary minerals that supersaturated at progressively lower temperatures would be removed from solution. As such, the observed groupings of major and trace elements support a model where hot spring fluids have re-equilibrated at progressively lower temperatures in Surprise Valley along an easterly-trending flow path.

Closer examination of concentration differences of specific elements in hot spring fluids compared to the reconstructed Phipps-2 sample also support progressive re-

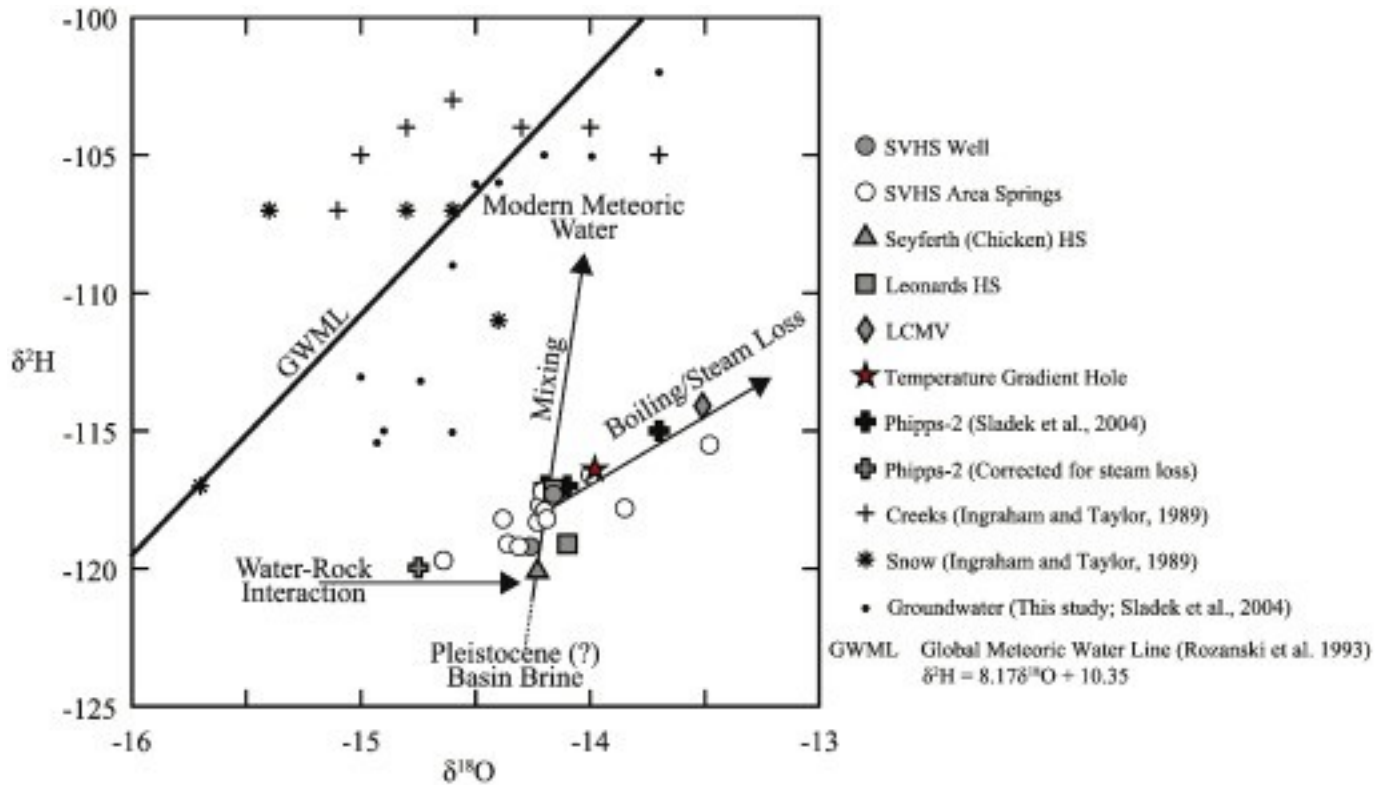
equilibration of Surprise Valley thermal fluids along an eastward flow path. Si solubility in geothermal fluids is temperature dependent with higher Si concentrations at elevated temperatures, and the formation of [silicate](#) minerals leads to lower Si concentrations in fluids during cooling and outflow ([White et al., 1956](#)). With increasing pH and progressively lower temperatures in Na-Cl geothermal waters (conditions that characterize hot springs in Surprise Valley), Ba and Sr partition into carbonate, Ca-bearing zeolites or major Ca-bearing [alteration mineral](#) phases, and Li, Rb and Cs are incorporated into [clay minerals](#) and zeolites ([Giggenbach and Goguel, 1989](#); [Kaasalainen and Stefánsson, 2012](#); [Kaasalainen et al., 2015](#)). The sample from Seyferth spring generally follows this pattern, but is anomalous from other eastern hot springs in that Sr and Ba concentrations approach those from the LCMV hot spring ([Fig. 6D](#)).

Carbonate [supersaturation](#) and precipitation in the subsurface (i.e. re-equilibration of fluids by secondary mineral formation) is also supported by the observation of large calcite blocks that were ejected from the LCMV during the 1951 mud volcano eruption. Calcite has a bladed [crystal](#) form in many of the blocks ([Table 4](#)), which is a typical product when near-neutral to alkaline geothermal fluids boil and CO₂ gas exsolves ([Browne, 1978](#); [Simmons and Christenson, 1994](#)). Assuming the LCMV calcite blocks formed from fluids with a similar $\delta^{18}\text{O}$ value to modern LCMV hot spring fluids, the maximum calculated boiling temperature in the subsurface when the calcite formed was 128 °C ([Table 5](#)). It cannot be confirmed, however, if the calcite formed at an earlier time from fluids with a different $\delta^{18}\text{O}$ value as the only age constraint is pre-1951. The calculated temperatures are, however, remarkably consistent with shallow subsurface temperatures measured in wells Parman 1 (140 °C) and Parman 2 (125 °C) that were drilled in the LCMV, and with the equilibration temperature of 132 °C computed in the GeoT re-equilibration model for LCMV ([Fig. 4A](#)). Evidence for persistent subsurface boiling and steam loss, as opposed to surface evaporation, comes from superheated conditions measured in one LCMV pond of 96.7 °C ([Sladek et al., 2004](#)) and 99 °C in August 2015 (this study), compared to the [boiling point](#) for pure water of 95.5 °C at the LCMV sample elevation of 1368 m. The superheated fluid temperature could result from the influx of steam that initially separated at a higher boiling temperature and pressure in the subsurface. The idea of subsurface boiling is further supported by the drilling history, where well Parman 3 was destroyed when drilling intercepted boiling fluids at a depth of 92 m.

4.4. Fluid stable isotope (δD and $\delta^{18}\text{O}$) and conservative element characteristics

Relationships between conservative elements in fluids that don't readily participate in temperature-dependent equilibrium reactions (e.g. Cl, B, F) provide a useful tool to identify geochemical processes that may influence hot spring compositions, and to further examine the dilution and re-equilibration models. [Duffield and Fournier \(1974\)](#) suggested that variable B and Cl concentrations in Surprise Valley hot spring fluids reflect variable dilution of geothermal fluids from a common source by low concentration [meteoric waters](#). Rather than dilution, [Sladek et al. \(2004\)](#) suggested that Surprise Valley springs undergo evaporative concentration at the ground surface owing to low flow rates and the arid climate, particularly at LCMV, which has the lowest flowrates of springs in the area (e.g. [Reed, 1975](#)). This idea was supported using binary plots of B vs. Cl and F vs. Cl, and showing that δD and $\delta^{18}O$ values for hot springs throughout Surprise Valley fall on an evaporation line. Evaporative modification has also been invoked to explain hot spring fluid [stable isotope](#) systematics in the similarly arid and nearby Klamath Basin ([Palmer et al., 2007](#)).

Fluid δD and $\delta^{18}O$ measurements form an evaporation line for SVHS area samples and Leonards Spring West samples. The evaporation line is defined at the isotopically heaviest (most evaporated) end by the sample from the LCMV spring and isotopically lightest end (least evaporated) by several samples from the SVHS area, and samples from Leonards Spring West (BLM) ([Fig. 8](#)). However, δD and $\delta^{18}O$ values of the sample from Seyferth spring are inconsistent with evaporation of a parent geothermal fluid. The Seyferth spring δD value ($\delta D = -120\text{‰}$) is the same as the corrected deep Phipps-2 fluid ($\delta D = -120\text{‰}$), when δD and $\delta^{18}O$ values in the [Sladek et al. \(2004\)](#) Phipps-2 sample are corrected for continuous steam loss from 180 °C (deep temperature) to 100 °C (sampling temperature) using the equations of [Truesdell et al. \(1977\)](#). Similar δD values of Phipps-2 and Seyferth fluids suggest they have a similar source fluid. The Seyferth spring $\delta^{18}O$ value ($\delta^{18}O = -14.3\text{‰}$) is somewhat heavier than the corrected deep Phipps-2 fluid ($\delta^{18}O = -14.8\text{‰}$), suggesting more extensive water-rock reaction for the Seyferth sample possibly owing to a longer outflow path ([Fig. 8](#)). Mixing of the Seyferth fluid with modern meteoric water could produce the measured [isotopic compositions](#) of other springs on the eastern side of the valley. This mixing relationship is reinforced by locations from which multiple samples were taken at different time periods (SVHS, Leonards Spring West (BLM), and several of the SVHS area springs), which trace the proposed mixing line in terms of δD and $\delta^{18}O$. This relationship supports the idea that the [mixing ratio](#) between a deep fluid and meteoric water varies seasonally, possibly in relation to increased [groundwater recharge](#) during spring [snowmelt](#) runoff.



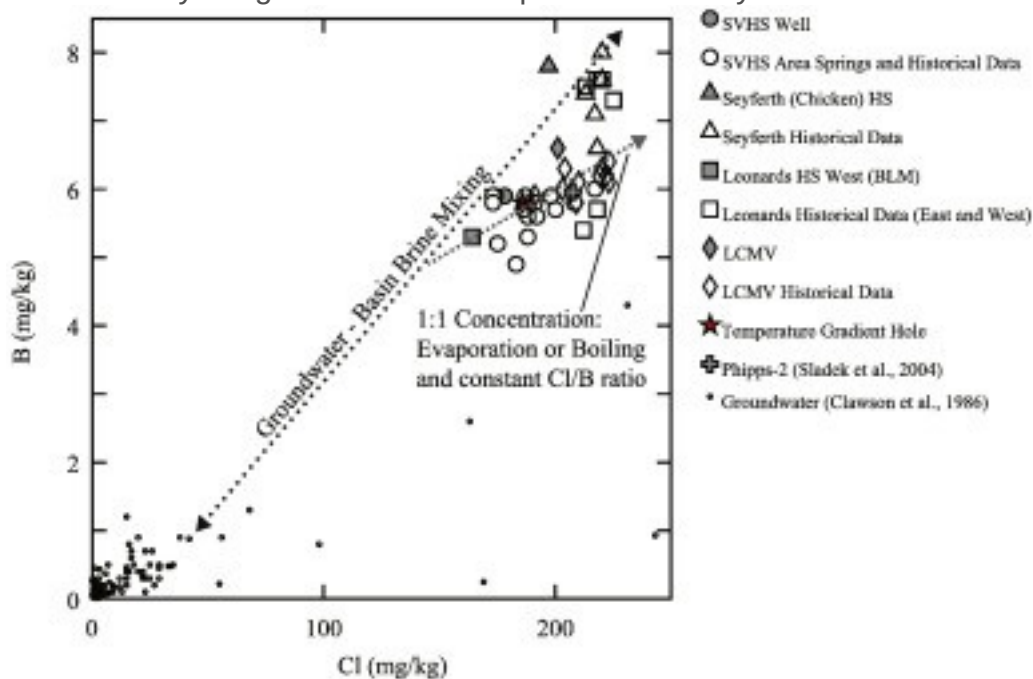
1. [Download high-res image \(276KB\)](#)
2. [Download full-size image](#)

Fig. 8. [Stable isotope](#) results for hot springs, thermal fluids and groundwater from [Table 4](#) of this study and Surprise Valley groundwater, creek, and snow samples from [Sladek et al. \(2004\)](#) and [Ingraham and Taylor \(1989\)](#). Many thermal fluids from the east side of the valley have lighter [deuterium](#) values than any meteoric source identified in Surprise Valley. Springs from the eastern side of the valley (SVHS, Leonards, and Seyferth) trace a mixing line between fluids with the lightest deuterium values and modern [meteoric water](#). Phipps-2 waters sampled by [Sladek et al. \(2004\)](#) fall on an evaporation/boiling trend owing to boiling in different parts of the sampling apparatus during sampling of ~180 °C fluid. LCMV, [CEC borehole](#), and a couple of springs in the SVHS area fall on an evaporation line. When oxygen and [hydrogen isotope](#) values for the Phipps-2 sample are corrected for continuous steam loss between 180 °C and 100 °C using the equations of ([Truesdell et al., 1977](#)), the resulting values are similar to those in the isotopically lightest samples collected in this study.

GWML from [Rozanski et al. \(1993\)](#).

This interpretation of isotopic data is also supported by B and Cl concentrations. A binary plot of B and Cl concentrations measured in this and previous studies shows two distinctive trends. B and Cl concentrations in Seyferth and Leonards Spring East are distinctively high, while SVHS, Leonards Spring West (BLM), and LCMV spring fluids fall

on a line with a 1:1 slope (Fig. 9). This linear trend formed by SVHS, Leonards Spring West, and LCMV suggests a relationship of evaporative concentration between these three fluids. By contrast, B and Cl concentrations in Seyferth and Leonards Spring East do not plot on this line, and instead form a cluster of higher B/Cl ratios. When considered along with the isotopic data, Seyferth fluids appear to have interacted with relatively less meteoric fluid. The interpretation that other fluids in the valley may be influenced by a mixture of Seyferth fluids and meteoric fluids is supported by the intersection of the B/Cl evaporation line with this Seyferth-meteoric fluid mixing line. The intersection of this evaporation line at an intermediary point on the primary mixing line suggests that fluids emerging in the west (Leonards, LCMV, and SVHS) may be influenced by a higher meteoric component than Seyferth and Leonards.



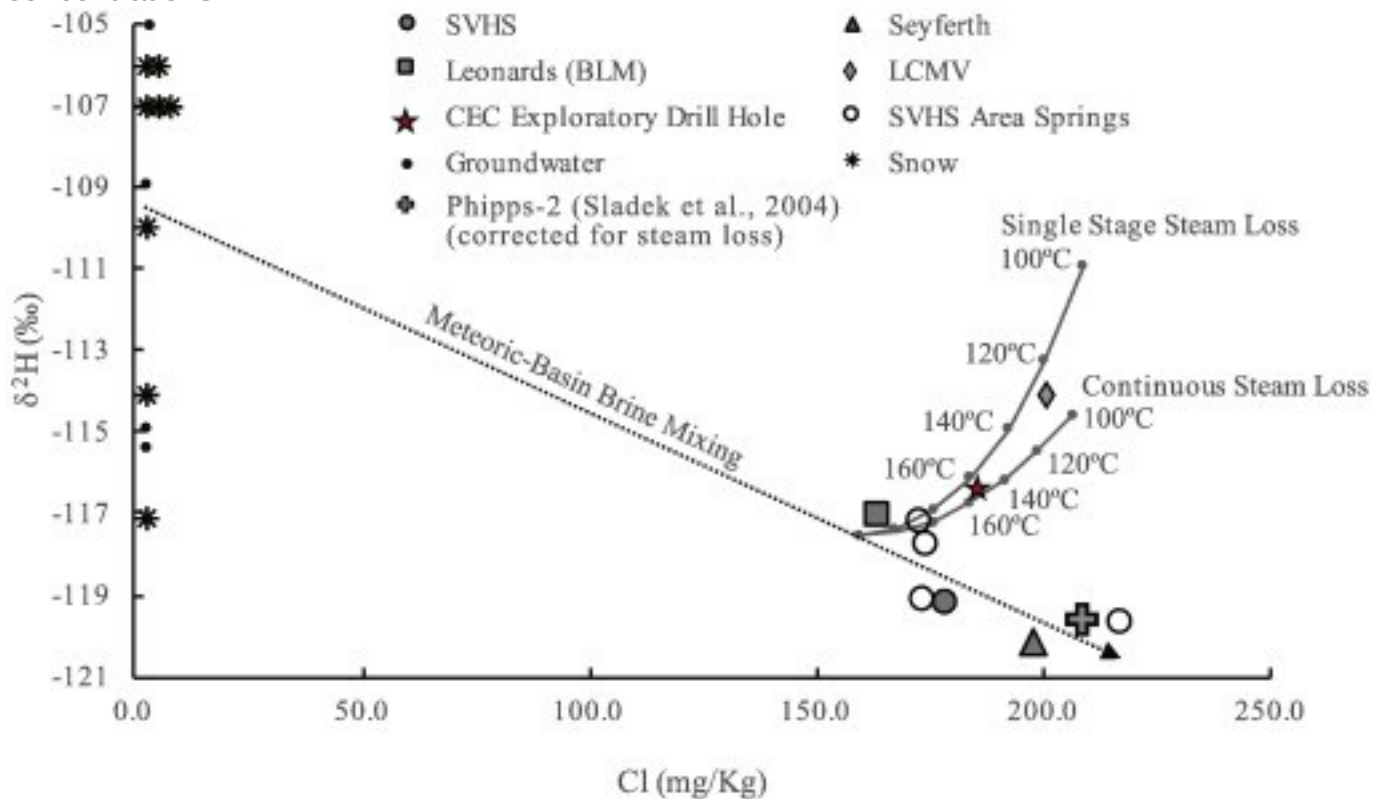
1. [Download high-res image \(197KB\)](#)
2. [Download full-size image](#)

Fig. 9. Data from this study (grey symbols) coupled with a compilation of historic hot spring fluid data (open symbols), including a deep subsurface sample (corrected for steam loss) from the Phipps-2 well.

Historical data from: ([Duffield and Fournier, 1974](#); [Reed, 1975](#); [Bliss, 1983](#); [Clawson et al., 1986](#); [Sladek et al., 2004](#)).

A model of deep brine dilution by meteoric water is not necessarily inconsistent with the low temperature re-equilibration model, or counter to the assertion that high dilution factors required for equilibrium with a high temperature mineral assemblage are unrealistic. A plot of δD and Cl ([Fig. 10](#)) traces a mixing line between modern meteoric

water and a brine with similar δD and Cl values to Seyferth spring, Spring X, and the reconstructed deep fluid from Phipps-2, which are proposed to approximate the δD and Cl of the parent geothermal fluid. The LCMV fluid cannot be related back to the parent geothermal fluid by direct dilution or evaporation, but could result from boiling of a mixture between the deep brine and modern meteoric water (Fig. 10). This relationship requires that mixing occurred prior to boiling rather than in the shallow subsurface at the end of the flow path and emergence of the hot spring. Therefore, mixing between a brine and modern meteoric water was not necessarily the final modification to hot spring fluids, but conceivably occurred in the deep subsurface prior to temperature-dependent equilibration with rocks and the formation of secondary minerals that initially set element concentrations.



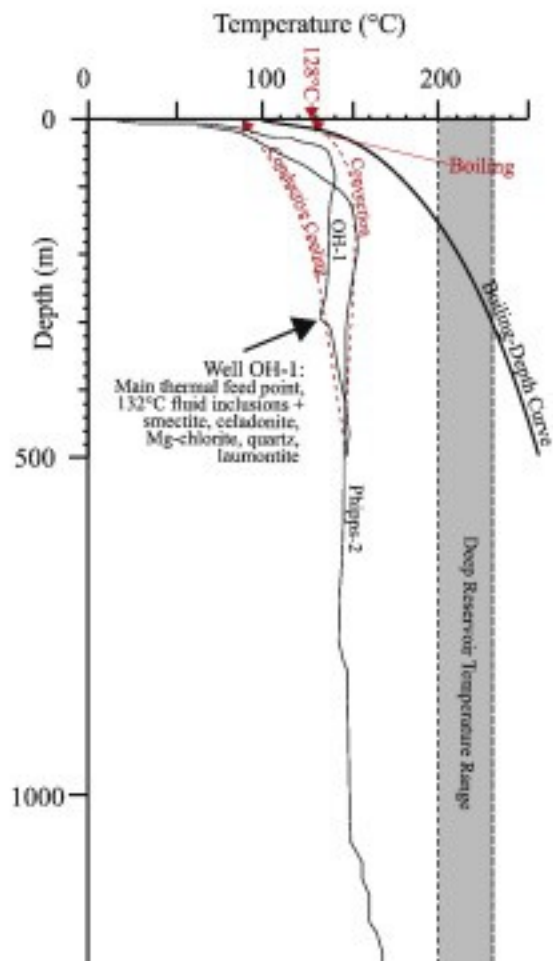
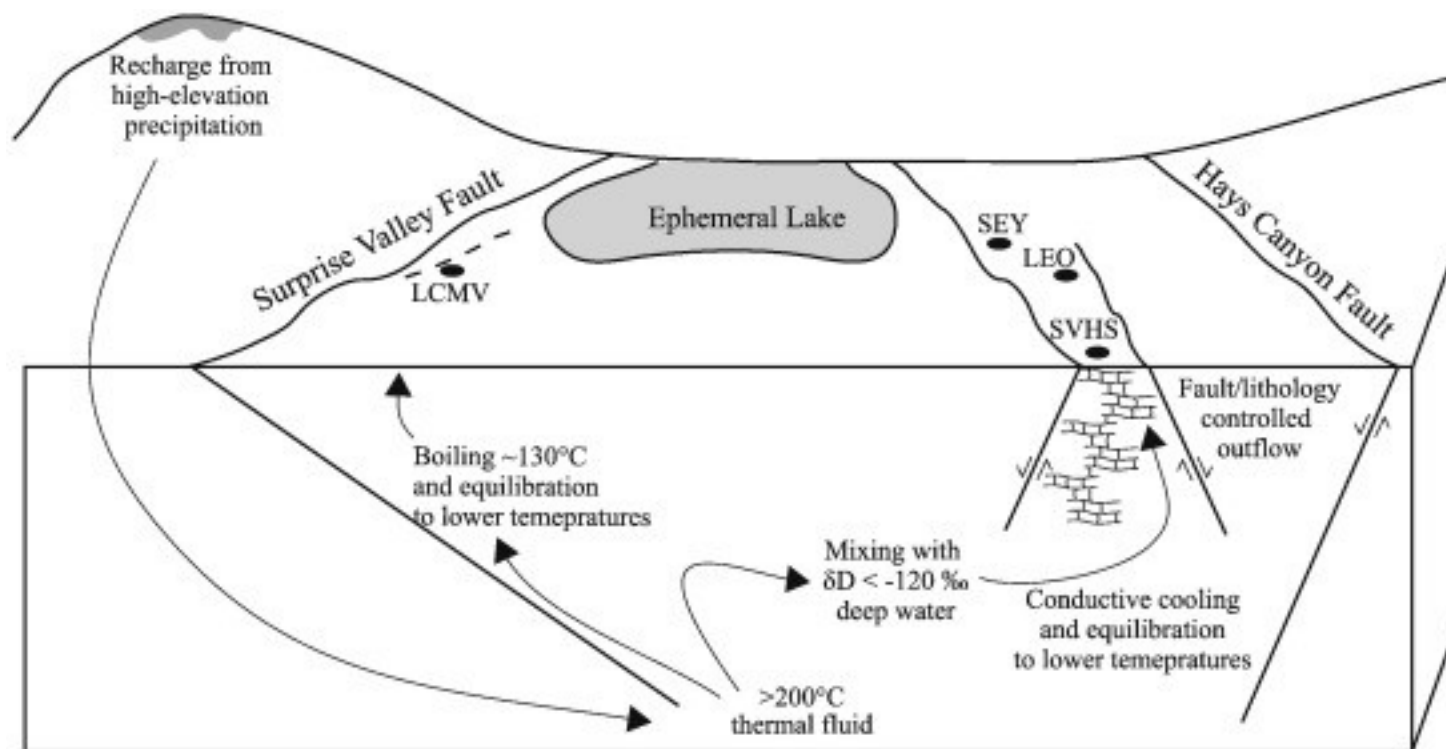
1. [Download high-res image \(247KB\)](#)
2. [Download full-size image](#)

Fig. 10. The deuterium-chloride relationship for Surprise Valley thermal fluids and [meteoric waters](#) support a model where the thermal fluid source has [deuterium](#) values lighter than any meteoric or snow source identified in the valley. A mixture of this isotopically light fluid and modern meteoric water boils to produce fluids in the [CEC](#) exploratory [borehole](#) and LCMV fluids. Curves are shown for evolution of a hypothetical fluid arbitrarily assigned values of $\delta D = -117.5$ and Cl = 160 ppm through

single stage steam loss and continuous steam loss from 220 °C to 100 °C, based on the equations of [Truesdell et al. \(1977\)](#). The deuterium value for the Phipps-2 sample is corrected for continuous steam loss from 180 °C to 100 °C using the equation of [Truesdell et al. \(1977\)](#), and Cl is corrected for 11% steam loss. The result shows the Phipps-2 sample falls near the isotopically lightest thermal fluids sampled in the valley. As noted earlier, some of the Surprise Valley [thermal waters](#) have δD values that are lower than any of the local non-thermal groundwater or recent precipitation sources. Similar discrepancies have been noted between geothermal fluids and non-thermal waters in other basins within the Basin and Range Province. This shift has been interpreted to indicate that the geothermal fluids represent recharge from Pleistocene waters. Such waters would be depleted in [deuterium](#) relative to modern-day precipitation due to cooler climatic conditions (e.g. [Mariner et al., 1983](#); [Flynn and Buchanan, 1990](#); [Smith, 2002](#)). In Surprise Valley, this deep water is ubiquitously associated with thermal features, and geologic structures that transmit thermal fluids to the ground surface. Indeed, this Pleistocene brine is probably synonymous with the thermal fluid signature in groundwater samples identified by ([Fowler et al., 2017](#)) using statistical methods.

4.5. Conceptual model of the Surprise Valley geothermal system

As noted earlier, deep thermal temperature estimates based on dissolved sulfate–water oxygen isotope exchange temperatures for Surprise Valley hot spring waters and multicomponent geothermometry applied to the Phipps-2 sample predict maximum reservoir temperatures in the 200 to 228 °C range ([Reed, 1975](#); [Nehring et al., 1979](#); [Fowler et al., 2015](#)). This is somewhat higher than the maximum temperature of 170 °C measured at the base of the Phipps-2 well ([Fig. 11](#)). It is not possible to extrapolate temperature gradient hole and Phipps-2 [temperature profiles](#) and estimate the depth to the hotter estimated temperatures, as the temperatures profiles have a near-vertical convective character at the base ([Fig. 11](#)). If a hotter reservoir is present vertically below the Phipps-2 and temperature gradient wells, it is possible that it is partially isolated from shallower convective fluids in the Phipps-2 by a low permeability unit. Alternatively, Phipps-2 and other temperature gradient holes may be laterally offset from a higher temperature zone with focused upflow closer to, or directly below, the LCMV. In this scenario, Phipps-2 and temperature gradient holes may sample the slightly cooled outflow from the main reservoir that has flowed laterally along the Surprise Valley Fault. The location and depth of the hottest fluids in Surprise Valley remain speculative.



1. [Download high-res image \(501KB\)](#)
2. [Download full-size image](#)

Fig. 11. Conceptual model for the Surprise Valley [geothermal system](#). Angles, depths, and distances are for illustrative purposes only. Potential [temperature profiles](#) of fluids emerging at LCMV (Lake City Mud Volcano) on the western side of the valley and SVHS, SEY and [LEO](#) (Surprise Valley Hot Spring, Seyferth hot spring and Leonards hot spring) on the eastern side of the valley that are compatible with fluid geochemical and [stable isotope](#) measurements are shown in the lower diagram. Faults are simplified from ([Egger et al., 2014](#)). [Fluid inclusion](#) and mineral data from [Moore and Segall \(2005\)](#); Phipps-2 well and OH-1 temperature gradient hole static temperature curve from [Benoit et al. \(2005b\)](#).

Processes influencing fluid compositions on leaving the deeper reservoir are better constrained. The overall picture for Surprise Valley geothermal fluids based on spring water compositional and stable isotope data coupled with optimized multicomponent geochemical modeling is: 1) Variable (seasonal) mixing between modern meteoric water and an older, deep thermal brine sourced during a time meteoric fluids had lower deuterium values followed by equilibration with rocks at elevated temperatures; 2) at LCMV, boiling of the mixed fluid around 130 °C, precipitation of calcite, and [exsolution](#) of CO₂; and 3) along an eastward flow path, equilibration of the mixed fluids without boiling at progressively lower temperatures through conductive cooling, little or no exsolution of CO₂, loss of several elements probably to silicate, carbonate and clay mineral formation, and emergence as hot springs on the eastern side of Surprise Valley. This model is summarized in [Fig. 11](#), which shows different boiling with depth relationships. This model implies that assumptions of equilibrium with quartz or feldspar may not apply to surface hot spring samples from Surprise Valley. The implication is that classical geothermometry estimates of the maximum temperature of the Surprise Valley [geothermal resource](#) applied to hot spring fluid samples are unreliable.

The idea of subsurface boiling at LCMV has implications for the driving force behind the 1951 LCMV eruption, and earlier eruptions that were hypothesized by [White \(1955\)](#). Over-pressurization of a subsurface boiling system likely triggered the LCMV eruption, a mechanism commonly responsible for hydrothermal eruptions elsewhere (e.g. [Browne and Lawless, 2001](#)). The cause for over-pressurization is speculative and requires focused study, but here we provide some intriguing possibilities. The receding Pleistocene Lake Surprise ([Ibarra et al., 2014](#)) may have reduced [confining pressure](#) and led to periodic eruptions. Increased demands on groundwater supplies for irrigation that reduced pressure from an overlying [aquifer](#) is another a potential cause of

the eruption. Explosive hydrothermal features can present hazards to human life (e.g. [Escobar Bruno et al., 1992](#)). Determining the triggering mechanism for the 1951 LCMV eruption is beyond the scope of this study, but a developing a conceptual model of the geothermal system provides a foundation for future investigations focused on possible climatic and anthropogenic influences on hydrothermal hazards.

5. Conclusions

A conceptual geochemical model of the Surprise Valley [geothermal system](#) is presented. The model is supported by multicomponent [geothermometry](#) models, as well as compositional and [stable isotope](#) measurements of hot spring fluids. Multicomponent geothermometry models are compatible with fluid re-equilibration after emergence from a hotter source by the formation of [silicate minerals](#) (clays, [zeolites](#) and cristobalite) and [calcium carbonate](#) during outflow at temperatures lower than about 132 °C. Model equilibration temperatures are supported by [oxygen isotope](#) exchange temperatures calculated from samples of LCMV [spring waters](#) and [calcite](#) blocks ejected from 1951 LCMV eruption. Fluid stable isotope (δD and $\delta^{18}\text{O}$) results suggest LCMV area fluids boiled and lost steam in the subsurface, while fluids on the eastern side of the valley did not boil, cooled conductively, and equilibrated at lower temperatures along an eastward flow path. These results are consistent with models of [structural control](#) on [fluid flow](#) proposed by [Egger et al. \(2014\)](#) and [Fowler et al. \(2017\)](#), whereby the principal geothermal upflow zone is related to the SVF on the western side of the valley near the LCMV, and outflow to the eastern side of the valley is controlled by a distinct fault that intersects the SVF at depth. δD values for hot spring fluids are at least 3 to 4‰ lighter than any modern [meteoric water](#) source in Surprise Valley, and require a Pleistocene groundwater component. This deep component is best represented by the sample from Seyferth hot spring, which would suggest the Pleistocene groundwater has elevated total dissolved solids, likely from prolonged [water/rock interaction](#). The implication of the proposed conceptual model is that the maximum temperature of the Surprise Valley [geothermal resource](#) is poorly constrained by classical geothermometers applied to hot spring compositions. We suggest that results for the dissolved sulfate oxygen isotope geothermometer ([Reed, 1975](#)) and multicomponent geothermometry results applied to deep fluids corrected for steam loss ([Fowler et al., 2015](#)), which suggest maximum subsurface temperatures in the 200 °C to 228 °C range, provide more robust estimates for deep reservoir temperatures at Surprise Valley than classical geothermometry methods.

Acknowledgements

All data for this paper is properly cited and referred to in the reference list. The data necessary to reproduce this work are included in tables. Any additional data or source files are available from the authors upon request (afowler@umn.edu). REE analysis was supported by the U.S. Department of Energy Grant [EE00006748](#). N. Spycher and P. Dobson were supported by the U.S. Department of Energy, Office of [Energy Efficiency](#) and Renewable Energy(EERE), Geothermal Technologies Office (GTO) under Contract No. [DEAC02-05CH11231](#) with Lawrence Berkeley National Laboratory. This research was undertaken through a subcontract from the County of Modoc, State of California, for California Energy Commission Contract GRDA# GEO14003. We thank the Parman family, Rose family, and Jana Bennett for allowing access to their property for sampling. This work could not have been completed without their hospitality and support.

References

[Athens et al., 2016](#)

N.D. Athens, J.M.G. Glen, S.L. Klemperer, A.E. Egger, V.C. Fontiveros **Hidden intrabasin extension: evidence for dike-fault interaction from magnetic, gravity, and seismic reflection data in Surprise Valley, northeastern California**

Geosphere, 12 (1) (2016), pp. 15-25

[CrossRefView Record in Scopus](#)

[Barker et al., 2005](#)

B. Barker, M. Kennedy, M. Hoversten, M.C. van Soest, K. Williams **Geothermal exploration at Fort Bidwell, California**

Proceedings of the Thirtieth Workshop on Geothermal Reservoir Engineering, Stanford University, California (2005)

(January 31–February 2, 2005)

[Battistel et al., 2014](#)

M. Battistel, S. Hurwitz, W. Evans, M. Barbieri **Multicomponent geothermometry applied to a medium-low enthalpy carbonate-evaporite geothermal reservoir**

Energy Procedia, 59 (2014), pp. 359-365

[ArticleDownload PDFView Record in Scopus](#)

[Bau, 1991](#)

M. Bau **Rare-earth mobility during hydrothermal and metamorphic fluid-rock interaction and the significance of the oxidation state of europium**

Chem. Geol., 93 (1991), pp. 219-230

[ArticleDownload PDFView Record in Scopus](#)

[Benoit et al., 2004](#)

D. Benoit, C. Goranson, S. Wesnousky, D.D. Blackwell **Overview of the Lake City, California geothermal system**

Geotherm. Resour. Council Trans., 28 (2004), pp. 311-315

[View Record in Scopus](#)

[Benoit et al., 2005a](#)

D. Benoit, D.D. Blackwell, L. Capuano, C. Goranson, J.N. Moore, D. Carey **Phase 2 and 3 Slim Hole Drilling and Testing at the Lake City, California Geothermal field, AMP Resources (Surprise Valley), LLC**

(2005)

[Benoit et al., 2005b](#)

D. Benoit, J.N. Moore, C. Goranson, D.D. Blackwell **Core hole drilling and testing at the Lake City, California geothermal field**

Geotherm. Resour. Council Trans., 29 (2005), pp. 203-208

[View Record in Scopus](#)

[Bliss, 1983](#)

J.D. Bliss **Basic Data for Thermal Springs and Wells as Recorded in GEOTHERM, Part A. USGS Open File Report 83-428A, July 1983**

(1983)

[Browne, 1978](#)

P.R.L. Browne **Hydrothermal alteration in active geothermal fields**

Annu. Rev. Earth Planet. Sci., 6 (1978), pp. 229-248

[CrossRef](#)

[Browne and Lawless, 2001](#)

P.R.L. Browne, J.V. Lawless **Characteristics of hydrothermal eruptions, with examples from New Zealand and elsewhere**

Earth-Sci. Rev., 52 (2001), pp. 299-331

[ArticleDownload PDFView Record in Scopus](#)

[Cantwell and Fowler,](#)

[2014](#)

C.A. Cantwell, A.P.G. Fowler **Fluid geochemistry of the Surprise Valley geothermal system**

Proceedings of the Thirty-Ninth Workshop on Geothermal Reservoir Engineering. Stanford

University, California (2014)

(February 24–26, 2014)

[Clawson et al.,](#)

[1986](#)

R.F. Clawson, L.R. Gibson, S.L. Beach **Surprise Valley Ground Water Basin Study, California Department of Water Resources**

(1986)

[Coppin
et al.,
2002](#)

F. Coppin, G. Berger, A. Baur, S. Castet, M. Loubet **Sorption of lanthanides on smectite and kaolinite**

Chem. Geol., 182 (2002), pp. 57-68

[ArticleDownload PDFView Record in Scopus](#)

[D
e
b
r
u
y
n
e
-
e
t
-
a
l
:
:
:
:
:
2
0
1
6](#)

D. Debruyne, N. Hulsbosch, P. Muchez **Unraveling rare earth element signatures in hydrothermal carbonate minerals using a source–sink system**

Ore Geol. Rev., 72 (2016), pp. 232-252

[ArticleDownload PDFView Record in Scopus](#)

[Doherty,
2008](#)

J. Doherty **PEST–model-independent parameter estimation**

Water-mark Numerical Computing, Corinda 4075, Brisbane, Australia (2008)

<http://www.sspa.com/pest/>

[Duffield and
Fournier, 1974](#)

W.A. Duffield, R.O. Fournier **Reconnaissance Study of the Geothermal Resources of Modoc County, California. USGS Open File Report**

(1974), pp. 74-1024

[View Record in Scopus](#)

[Duffield and McKee, 1986](#)

W.A. Duffield, E.H. McKee **Geochronology, structure, and basin-range tectonism of the Warner Range, northeastern California**

Geol. Soc. Am. Bull., 97 (2) (1986), pp. 142-146

[CrossRefView Record in Scopus](#)

[Egger et al., 2011](#)

A.E. Egger, J.M.G. Glen, D.A. Ponce **The northwestern margin of the basin and range province**

Tectonophysics, 488 (1–4) (2010), pp. 150-161

[ArticleDownload PDFView Record in Scopus](#)

[Egger et al., 2011](#)

A.E. Egger, J.M.G. Glen, D.K. McPhee **Structural controls on geothermal circulation in Surprise Valley, California: a re-evaluation of the Lake City fault zone**

Geol. Soc. Am. Bull., 126 (3–4) (2014), pp. 523-531

[CrossRefView Record in Scopus](#)

[Escobar Bruno et al., 2014](#)

C.A. Escobar Bruno, J.A. Burgos, M.S. Ayala **Agua Shuca hydrothermal eruption**

GRC Bull. (1992), pp. 361-369

[Finsterle and Zhang, 2011](#)

S. Finsterle, Y. Zhang **Solving iTOUGH2 simulation and optimization problems using the PEST protocol**

Environ. Model. Softw., 26 (7) (2011), pp. 959-968

[ArticleDownload PDFView Record in Scopus](#)

[Flynn and Buchanan, 1990](#)

T. Flynn, P.K. Buchanan **Geothermal Fluid Genesis in the Great Basin. Final Report for the Period 1 August 1988–1 May 1990. Prepared for the U.S. Department of Energy, Idaho Operations Office under Contract DE-FG07-88ID12784**

(1990)

(154 pp)

[Fouillac and Michard, 1981](#)

C. Fouillac, G. Michard **Sodium/lithium ratio in water applied to geothermometry of geothermal reservoirs**

Geothermics, 10 (1) (1981), pp. 55-70

[ArticleDownload PDFView Record in Scopus](#)

[Fournier, 1977](#)

R.O. Fournier **Chemical geothermometers and mixing models for geothermal systems**
Geothermics, 5 (1977), pp. 41-50

[ArticleDownload PDFView Record in Scopus](#)

[Fournier, 1979](#)

R.O. Fournier **A revised equation for the Na/K geothermometer**
Geotherm. Resour. Council Trans., 3 (1979), pp. 221-224

[View Record in Scopus](#)

[Fournier and Tru](#)

R.O. Fournier, A.H. Truesdell **An empirical Na-K-Ca geothermometer for natural waters**
Geochim. Cosmochim. Acta, 37 (1973), pp. 1255-1275

[ArticleDownload PDFView Record in Scopus](#)

[Fournier and Pot](#)

R.O. Fournier, R.W. Potter II **An equation correlating the solubility of quartz in water from 25 to 900 C at pressures up to 10,000 bars**

Geochim. Cosmochim. Acta, 46 (10) (1982), pp. 1969-1973

[ArticleDownload PDFView Record in Scopus](#)

[Fowler and Ziere](#)

A.P.G. Fowler, R. Zierenberg

Rare earth element concentrations in geothermal fluids and epidote from the Reykjanes geothermal system, Iceland, Proceedings of the World Geothermal Congress, Melbourne, Australia (2015)

(19–25 August 2015)

[Fowler et al., 2015](#)

A.P.G. Fowler, C.A. Cantwell, N. Spycher, D. Siler, P.F. Dobson, M. Kennedy, R. Zierenberg **Integrated geochemical investigations of Surprise Valley thermal springs and cold waters**
PROCEEDINGS, Fourtieth Workshop on Geothermal Reservoir Engineering Stanford University, Stanford, California, January 26–28, 2015 (2015)

[Fowler et al., 2015](#)

A.P.G. Fowler, N. Spycher, R. Zierenberg, C.A. Cantwell **Identification of blind geothermal resources in Surprise Valley, CA, using publicly available groundwater well water quality data**

Appl. Geochem., 80 (2017), pp. 24-48

[ArticleDownload PDFView Record in Scopus](#)

[Friedman and O](#)

I. Friedman, J.R. O'Neil **Data of geochemistry**

Chapter KK. Compilation of Stable Isotope Fractionation Factors of Geochemical Interest. U.S. Geological Survey Professional Paper 440-KK (6th Edition) (1977)

[Giggenbach, 198](#)

W.F. Giggenbach **Geothermal solute equilibria. Derivation of Na-K-Mg-Ca geothermometers**

Geochim. Cosmochim. Acta, 52 (1988), pp. 2749-2765

[ArticleDownload PDFView Record in Scopus](#)

[Giggenbach and](#)

W.F. Giggenbach, R.L. Goguel **Collection and Analysis of Geothermal and Volcanic Water and Gas Discharges. DSIR Report CD 2401**

(4th edition) (1989)

Petone, New Zealand

[Glen et al., 2008](#)

J.M.G. Glen, A.E. Egger, D.A. Ponce **Structures controlling geothermal circulation identified through gravity and magnetic transects, Surprise Valley, California, Northwestern Great Basin**

Geotherm. Resour. Council Trans., 32 (2008), pp. 279-283

[Glen et al., 2013](#)

J.M.G. Glen, A.E. Egger, C. Ippolito, N. Athens

Correlation of geothermal springs with sub-surface fault terminations revealed by high-resolution, UAV-acquired magnetic data, Proceedings, Thirty-Eighth Workshop on Geothermal Reservoir Engineering, Stanford University, Stanford, California (2013)

February 11–13, 2013

[Godwin et al., 19](#)

L.H. Godwin, L.B. Haigler, R.L. Rious, D.E. White, L.J.P. Muffler, R.G. Wayland **Classification of public lands valuable for geothermal steam and associated geothermal resources**

United States Geological Survey Circular 647 (1971)

(18 pp)

[Hawkes et al., 20](#)

S.J. Hawkes, J.S. McClain, A. Kahn, K. Lewis **Using Electromagnetic Techniques to Test Models for Shallow Permeability in the Surprise Valley, CA Geothermal System. Abstract GP51C-1106, 2013 Fall Meeting, AGU**

(2013)

[Ibarra et al., 201](#)

D.E. Ibarra, A.E. Egger, K.L. Weaver, C.R. Harris, K. Maher **Rise and fall of late Pleistocene pluvial lakes in response to reduced evaporation and precipitation: evidence from Lake Surprise, California**

Geol. Soc. Am. Bull., 126 (11–12) (2014), pp. 1387-1415

[CrossRefView Record in Scopus](#)

[Ingraham and Ta](#)

N.L. Ingraham, B.E. Taylor **Hydrogen isotope study of large-scale meteoric water transport in northern California and Nevada**

J. Hydrol., 85 (1986), pp. 183-197

[ArticleDownload PDFView Record in Scopus](#)

[Ingraham and Ta](#)

N.L. Ingraham, B.E. Taylor **The effect of snowmelt on the hydrogen isotope ratios of creek discharge in Surprise Valley, California**

J. Hydrol., 106 (1989), pp. 233-244

[ArticleDownload PDFView Record in Scopus](#)

[Kaasalainen and](#)

H. Kaasalainen, A. Stefánsson **The chemistry of trace elements in surface geothermal waters and steam, Iceland**

Chem. Geol., 330-331 (2012), pp. 60-85

[ArticleDownload PDFView Record in Scopus](#)

[Kaasalainen et a](#)

H. Kaasalainen, A. Stefánsson, N. Giroud, S. Arnórsson **The geochemistry of trace elements in geothermal fluids, Iceland**

Appl. Geochem., 62 (2015), pp. 207-223

[ArticleDownload PDFView Record in Scopus](#)

[Kell-Hills et al., 2](#)

A. Kell-Hills, M. Thompson, M. Dhar, J. Louie, S. Pullammanappallil **A study of the Surprise Valley Fault using a high-resolution shallow seismic reflection profile**

Geotherm. Resour. Council Trans., 33 (2009), pp. 477-480

[Kerstel et al., 19](#)

E.R. Kerstel, R. van Trigt, N. Dam, J. Reuss, H.A.J. Meijer **Simultaneous determination of the 2H:1H, 17O:16O and 18O:16O isotope abundance ratios in water by means of laser spectrometry**

Anal. Chem., 71 (23) (1999), pp. 5297-5303

[CrossRefView Record in Scopus](#)

[Kharaka and Ma](#)

Y.K. Kharaka, R.H. Mariner **Chemical geothermometers and their application to formation waters from sedimentary basins**

Thermal history of sedimentary basins, Springer, New York, NY (1989), pp. 99-117

[CrossRefView Record in Scopus](#)

[King et al., 2016](#)

J.M. King, S. Hurwitz, J.B. Lowenstern, D.K. Nordstrom, R.B. McCleskey **Multireaction equilibrium geothermometry: a sensitivity analysis using data from the Lower Geyser Basin, Yellowstone National Park, USA**

J. Volcanol. Geotherm. Res., 328 (2016), pp. 105-114

[ArticleDownload PDFView Record in Scopus](#)

[LaFleur et al., 2010](#)

J. LaFleur, A. Carter, K. Moore, B. Barker, P. Atkinson, C. Jones, J.N. Moore, B. Paollard **Update on geothermal exploration at Fort Bidwell, Surprise Valley California**

Geotherm. Resour. Council Trans., 34 (2010), pp. 581-583

[Lerch et al., 2010](#)

D.W. Lerch, S.L. Klemperer, A.E. Egger, J.P. Colgan, E.L. Miller **The northwestern margin of the Basin-and-Range Province, part 1: reflection profiling of the moderate-angle (~30°) Surprise Valley Fault**

Tectonophysics, 488 (1–4) (2010), pp. 143-149

[ArticleDownload PDFView Record in Scopus](#)

[Mariner et al., 1983](#)

R.H. Mariner, T.S. Presser, W.C. Evans **Geochemistry of active geothermal systems in the northern Basin and Range province**

Geothermal Resources Council, Special Report No. 13, May 1983 (1983)

[Mariner et al., 1993](#)

R.H. Mariner, T.S. Presser, W.C. Evans **Geothermometry and water-rock interaction in selected thermal systems in the Cascade Range and Modoc Plateau, western United States**

Geothermics, 22 (1) (1993), pp. 1-15

[ArticleDownload PDFView Record in Scopus](#)

[Moore and Segall, 2005](#)

J.N. Moore, M. Segall **Hydrothermal alteration of the Surprise Valley reservoir rocks**

Energy and Geoscience Institute at the the University of Utah, Salt Lake City, Technical Report 54900900-7-30-05 (2005)

(40 pp)

[Nehring et al., 1979](#)

N.L. Nehring, R.H. Mariner, L.D. White, M.A. Huebner, E.D. Roberts, K. Harmon, P.A. Bowen, L. Tanner **Sulfate Geothermometry of Thermal Waters in the Western United States: USGS Open File Report 79-1135**

(1979), p. 10

[View Record in Scopus](#)

[O'Neil et al., 1969](#)

J.R. O'Neil, R.N. Clayton, T.K. Mayeda **Oxygen isotope fractionation in divalent metal carbonates**

J. Chem. Phys., 51 (12) (1969), pp. 5547-5558

[CrossRefView Record in Scopus](#)

[Palmer et al., 2007](#)

P.C. Palmer, M.W. Gannett, S.R. Hinkle **Isotopic characterization of three groundwater recharge sources and inferences for selected aquifers in the upper Klamath Basin of Oregon and California, USA**

J. Hydrol., 336 (1–2) (2007), pp. 17-29

[ArticleDownload PDFView Record in Scopus](#)

[Peiffer et al., 2014](#)

L. Peiffer, C. Wanner, N. Spycher, E.L. Sonnenthal, B.M. Kennedy, J. Iovenitti **Optimized multicomponent vs. classical geothermometry: insights from modeling studies at the Dixie Valley geothermal area**

Geothermics, 51 (2014), pp. 154-169

[ArticleDownload PDFView Record in Scopus](#)

[Quinn et al., 2006](#)

K.A. Quinn, R.H. Byrne, J. Schijf **Sorption of yttrium and rare earth elements by amorphous ferric hydroxide: influence of solution complexation with carbonate**

Geochim. Cosmochim. Acta, 70 (16) (2006), pp. 4151-4165

[ArticleDownload PDFView Record in Scopus](#)

[Reed, 1975](#)

M.J. Reed **Chemistry of thermal water in selected geothermal areas of California**

California Division of Oil and Gas, Sacramento, California (1975)

[Reed and Palandri, 2006](#)

M.H. Reed, J. Palandri **SOLTherm.H06, a Database of Equilibrium Constants for Minerals and Aqueous Species**

(2006)

(Available from the authors, University of Oregon, Eugene, Oregon)

[Reed and Spycher, 1984](#)

M. Reed, N. Spycher **Calculation of pH and mineral equilibria in hydrothermal waters with application to geothermometry and studies of boiling and dilution**

Geochim. Cosmochim. Acta, 48 (1984), pp. 1479-1492

[ArticleDownload PDFView Record in Scopus](#)

[Rigby and Zebal, 1981](#)

F.A. Rigby, G.P. Zebal **Case History on Geothermal-well-log Interpretation: Surprise Valley, California (No. LA-8598-MS)**

Los Alamos Scientific Lab, NM (USA) (1981)

[Rozanski et al., 1993](#)

K. Rozanski, L. Araguas-Araguas, R. Gonfiantini **Isotopic patterns in modern global precipitation**

Climate Change in Continental Isotopic Records. Geophysical Monograph, 78 (1993), pp. 1-36

[View Record in Scopus](#)

[Simmons and Christenson, 1994](#)

S.F. Simmons, B.W. Christenson **Origins of calcite in a boiling geothermal system**

Am. J. Sci., 294 (1994), pp. 361-400

[CrossRefView Record in Scopus](#)

[Sladek et al., 2004](#)

C. Sladek, G.B. Arehart, W.R. Benoit **Geochemistry of the Lake City geothermal system, California, USA**

Geotherm. Resour. Council Trans., 28 (2004), pp. 363-368

[View Record in Scopus](#)

[Smith, 2002](#)

G.I. Smith **Stable isotope compositions of waters in the Great Basin, United States 3. Comparison of groundwaters with modern precipitation**

J. Geophys. Res., 107 (D19) (2002)

[Spycher et al., 2014](#)

N. Spycher, L. Peiffer, E.L. Sonnenthal, G. Saldi, M.H. Reed, B.M. Kennedy **Integrated multicomponent solute geothermometry**

Geothermics, 51 (2014), pp. 113-123

[ArticleDownload PDFView Record in Scopus](#)

[Spycher et al., 2016](#)

N. Spycher, S. Finsterle, P.F. Dobson **New developments in multicomponent geothermometry**

Proceedings, 41st Workshop on Geothermal Reservoir Engineering, Stanford University, Stanford, California (2016)

(February 22–24, 2016)

[Tanner et al., 2016](#)

N. Tanner, C.D. Holt, S. Hawkes, J.S. McClain, L. Safford, L.L. Mink, C. Rose, R.A. Zierenberg **Investigation of Heat Source(s) of the Surprise Valley Geothermal System, Northern California. American Geophysical Union, Fall General Assembly 2016, abstract #NS31A-1948**

(2016)

[Truesdell et al., 1977](#)

A.H. Truesdell, M. Nathenson, R.O. Rye **The effects of subsurface boiling and dilution on the isotopic compositions of Yellowstone thermal waters**

J. Geochem. Explor., 82 (26) (1977), pp. 3694-3704

[CrossRefView Record in Scopus](#)

[White, 1955](#)

D.E. White **Violent mud-volcano eruption of Lake City hot springs, northeastern California**

Bull. Geol. Soc. Am., 66 (1955), pp. 1109-1130

[CrossRefView Record in Scopus](#)

[White et al., 1956](#)

D.E. White, W.W. Brannock, K.J. Murata **Silica in hot-spring waters**

Geochim. Cosmochim. Acta, 10 (1956), pp. 27-59

[ArticleDownload PDFView Record in Scopus](#)

[Woods, 1974](#)

M.C. Woods **Geothermal activity in surprise valley**

Calif. Geol., 27 (12) (1974), pp. 271-273

[View Record in Scopus](#)

[Zhu et al., 2010](#)

Y. Zhu, A. Itoh, T. Umemura, H. Haraguchi, K. Inagaki, K. Chiba **Determination of REEs in natural water by ICP-MS with the aid of an automatic column changing system**

J. Anal. At. Spectrom., 25 (8) (2010), pp. 1253-1258

[CrossRefView Record in Scopus](#)

1

Presently at the Department of Earth Sciences, University of Minnesota, Minneapolis, MN 55455, USA.